Spring 2021

# Investigation of post-acid stimulation impacts on well performance using fracture modeling and reservoir simulation in a Jurassic carbonate reservoir

Muaath Alansari

INVESTIGATION OF POST-ACID STIMULATION IMPACTS ON WELL PERFORMANCE USING FRACTURE MODELING AND RESERVOIR SIMULATION IN A JURASSIC CARBONATE RESERVOIR

by

MUAATH ALANSARI

A THESIS

Presented to the Graduate Faculty of the

MISSOURI UNIVERSITY OF SCIENCE AND TECHNOLOGY

In Partial Fulfillment of the Requirements for the Degree

MASTER OF SCIENCE IN PETROLEUM ENGINEERING

2021

Approved by:

Dr. Shari Dunn-Norman, Advisor
Mr. Larry K. Britt
Dr. Ding Zhu
Dr. Mingzhen Wei

# ABSTRACT

Well stimulation (well fracturing) became an essential tool in the Oil and Gas industry to unlock the potential of unconventional reservoirs all over the world and especially in the Middle East. In Kuwait, well stimulation is obligatory when dealing with deep Jurassic carbonate reservoirs. Thus, the well fracture designing process plays a very critical role in determining the success of the stimulation job and the improvement of the recovery.

Several wells stimulated with 20% HCL have shown wide variations in both short and long term well production performance. The research aims to investigate and identify the possible reasons causing these variations by creating an integrated workflow comprised of two modeling sections using actual field data. Fracture Modeling; to assess the fracturing operation and obtain the fracture geometry and conductivity using StimPlan software. Reservoir Simulation; to test the fracture design by the performance of the well using Petrel and Eclipse software. The iterative process in the workflow also gives the ability to tailor the design to reach the maximum potential of the well.

Three major reasons are suspected to be behind the underperformance of the investigated well. First, human errors in planning and gathering the required data for the stimulation job. Second, the stress contrast between the layers allows the fracture to propagate vertically giving more fracture height than length. Third, the fracture orientation, which has a great effect on the long-term performance by allowing the induced fracture to intersect with the formation and the natural fractures.

## ACKNOWLEDGMENTS

I sincerely would like to express my deepest gratitude to Dr. Shari Dunn-Norman, whom I consider as a family member not only my mentor and advisor, for her continuous support and guidance during the past three years along with my undergraduate years, and I wish in the near future to pursue my PhD degree as her student. I also wish to show my gratitude and appreciation to Dr. Larry Britt for lending me his valuable time and expertise throughout the fracture modeling part. I like to extend my deepest appreciation to my committee members, Dr. Ding Zhu and Dr. Mingzhen Wei, for their assistance, encouragement, and valuable research resources.

I wish to thank Kuwait Petroleum Corporation (KPC) and Kuwait Oil Company (KOC) for giving me the opportunity to attain this achievement. I want to thank the Missouri University of Science & Technology for all the support and for making me feel at home.

I would like to pay my special regards to my friends and colleagues: Ahmad Alkanderi, Ali Waqar, Ibraheem Alzaidani, Mohammad Alsharrad, Mohammad Jumaa, Mohammad Moosa, Mutlaq Alarouj, Saad Alajmi, Saleh Alsayegh, Taha Bloushi, Waleed Alquraini, and Yaser Alnaqi, for their continuous technical and emotional support.

Lastly, I would like to thank my beloved family, parents, brother, and sister for their patience and endless support during my time away from home.

# TABLE OF CONTENTS

## LIST OF ILLUSTRATIONS

Page

# LIST OF TABLES

# NOMENCLATURE

| Symbol | Description |
|---|---|
| M.Y. | Million Years |
| PSI | Pound Per Square Inch |
| F | Fahrenheit |
| mD | Millidarcy |
| FT | Feet |
| SPF | Shots Per Foot |
| $FT^3$ | Cubic Feet |
| API | American Petroleum Institute |
| PLT | Production Logging Tool |
| KBE | Kelly Bushing Elevation |
| MSL | Mean Sea Level |
| OBM | Oil Based Mud |
| KOP | Kick-Off Point |
| DST | Drill Stem Test |
| PBTD | Plug Back Total Depth |
| TCP | Tubing-Conveyed Perforating |
| BPF | Barrels Per Foot |
| MD | Measured Depth |
| TVD | Total Vertical Depth |
| PPF | Pounds Per Foot |

| | |
|---|---|
| HCL | Hydrochloric Acid |
| AI | Artificial Intelligence |
| DDFN | Deformable Discrete Fracture Network |
| KOC | Kuwait Oil Company |
| PI | Productivity Index |
| SPSP | Single Porosity Single Permeability |
| DPDP | Double Porosity Double Permeability |
| DFN | Discrete Fracture Network |
| PVT | Pressure Volume Temperature |
| ISIP | Instantaneous Shut-In Pressure |
| 1D | One Dimension |
| 3D | Three Dimension |
| BBL | Barrel |
| $F_{cd}$ | Dimensionless Fracture Conductivity |
| BPM | Barrels Per Minute |
| INCL | Inclination |
| DLS | Dogleg Severity |
| BHP | Bottom Hole Pressure |
| HM | History Matching |
| KH | Permeability x Thickness |
| STB/D | Stock Tank Barrel Per Day |
| MSCF/D | Thousand Standard Cubic Feet Per Day |
| CP | Centipoise |

| | |
|---|---|
| $P_{res}$ | Reservoir Pressure |
| $P_c$ | Closure Pressure |
| $T_c$ | Closure Time |
| K | Permeability |
| MIN | Minute |
| PPG | Pounds Per Gallon |
| IN | Inch |
| BBLS/MIN | Barrels Per Minute |
| $X_f$ | Fracture Half-Length |
| $H_f$ | Fracture Height |
| $W_f$ | Fracture Width |
| MSCF | Thousand Standard Cubic Feet |
| STB | Stock Tank Barrel |
| DEG | Degree |
| Q/C | Quality Check |

# 1. INTRODUCTION

## 1.1. BACKGROUND

The domestic demand for gas led Kuwait Oil Company to the discovery of the unconventional Jurassic age reservoirs. There are six main fields contributing to gas and light oil production. The biggest two fields are Sabriyah and Raudhatain shown in Figure 1.1 are the bread and butter for the Jurassic project, surrounded by Bahrah, Dhabi, Um-Niqqa, and North-West Raudhatain. Middle Marrat and Najmah-Sargelu formations are spreading across all the mentioned fields. Unlike the famous conventional sandstone Burgan field, the Jurassic reservoirs are highly fractured carbonate formations, and they are the only formations producing commercial quantities of hydrocarbons.


Figure 1.1 Map of Jurassic Fields Locations (www.kpc.com.kw).

The lithology of Najmah-Sargelu formation in Figures 1.2 and 1.3 is slightly different than Middle Marrat. It consists of a mix of limestone and kerogen layers, while Middle Marrat contains limestone, shale, anhydrite, and dolomites.

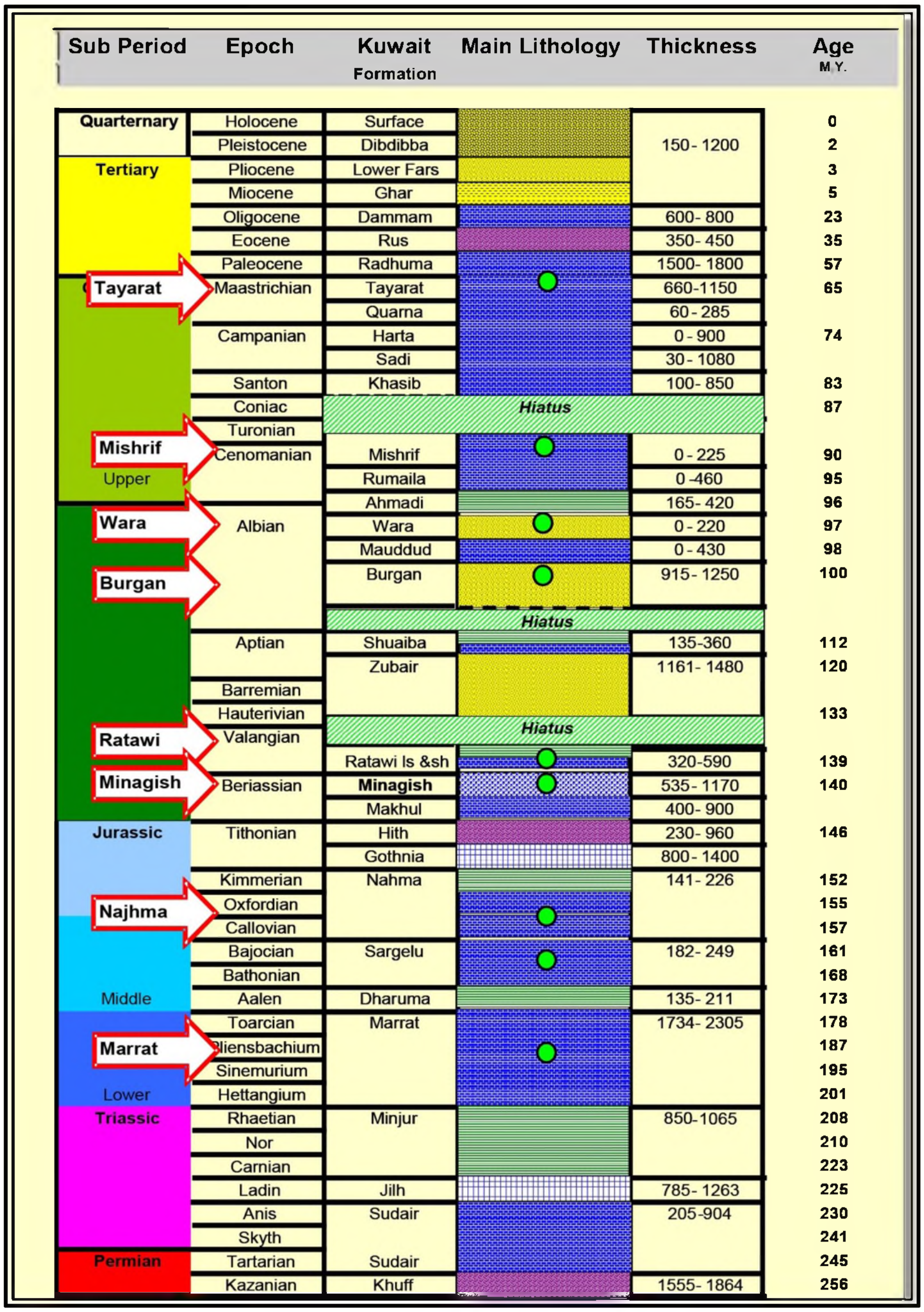


Figure 1.2 Kuwait Formations Geological Stratigraphy (Al-Muhailan et al., 2016).

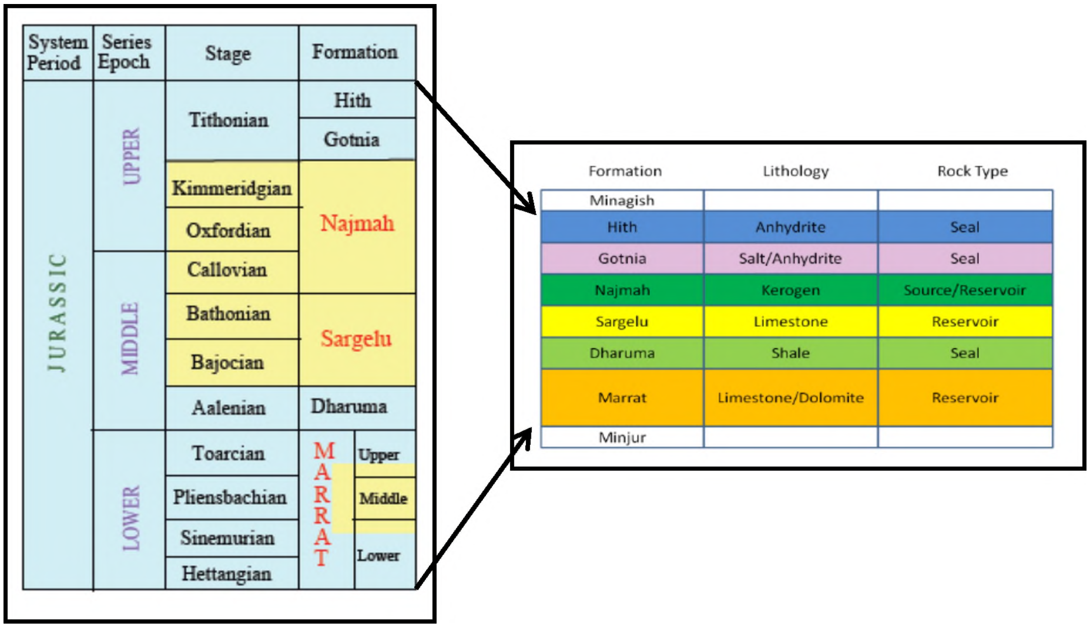


Figure 1.3 Jurassic Formations Rock Types.

The deep and sour environment raised many challenges in the journey of drilling and developing these complex reservoirs, which also contain near critical point fluids. A summary of the field's properties is listed in Table 1.1.

Table 1.1 Properties of Raudhatain Field.

| ***Raudhatain*** | |
|---|---|
| Reservoir | Middle Marrat |
| Initial Pressure | 11000 Psi |
| Reservoir Temperature | 270 F |
| Porosity | 15 - 20 % |
| Permeability | 0.0001 - 100 mD |
| Reservoir Fluid | Volatile Oil |
| Depth | ~ 16000 ft |
| $H_2S$ | ~ 1 % |
| $CO_2$ | ~ 0.3 % |

The subject of study in this research is MA-021, a well located on the west side of the Raudhatain field illustrated in Figure 1.4. It was drilled as a deviated well adapting the 7 casings policy for the completion design as demonstrated in Figure 1.5. In Middle Marrat formation in 2008, an overbalanced perforation was adopted using 6 spf with 45 degrees phasing. An illustration of the gun used for perforation is shown in Figure 1.6.

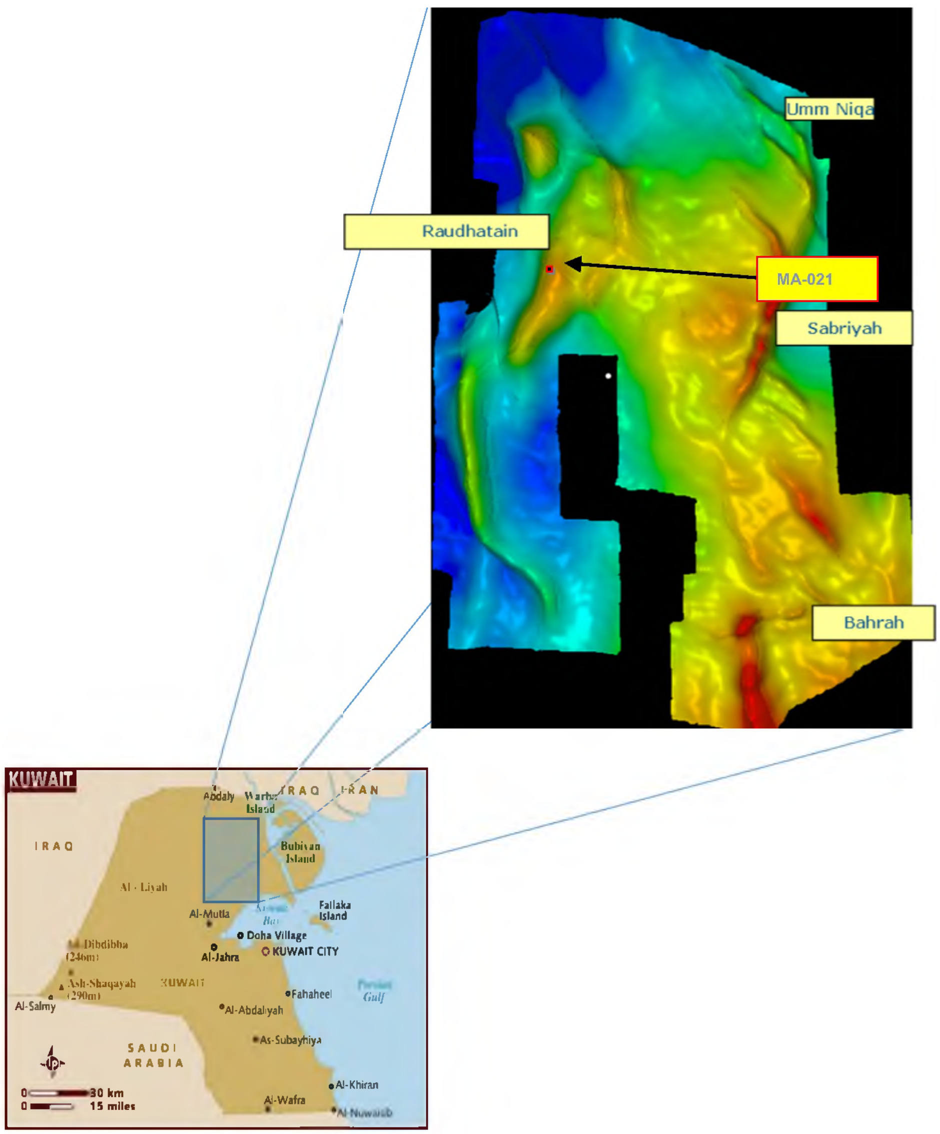


Figure 1.4 Well Location Map.

| KBE : 162 ft Above MSL | Mud wt: 17.8 ppg |
|---|---|
| G.Elevation :124 ft above MSL | Comp.fluid:Treated OBM |

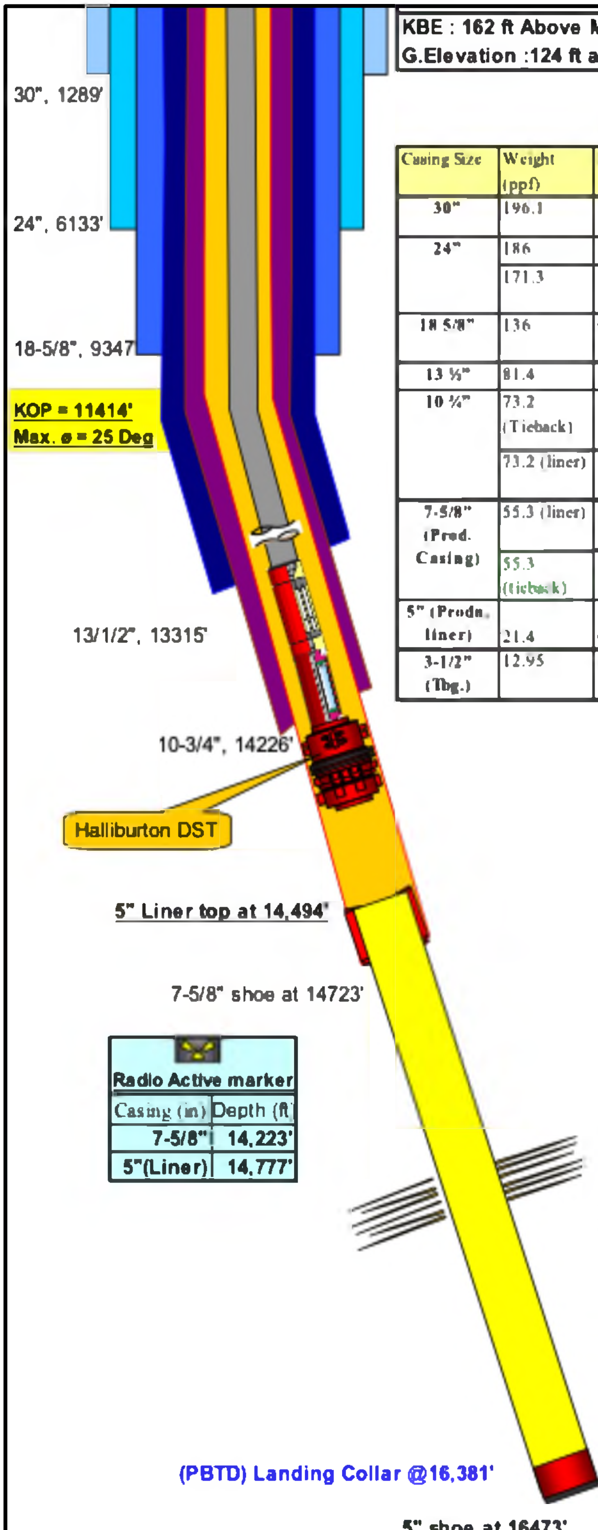


**Casing Data:**

| Casing Size | Weight (ppf) | Grade | Type | Setting Depth (ft) | Nom. ID | Drift ID | Capacity (bpf) |
|---|---|---|---|---|---|---|---|
| 30" | 196.1 | B | Vetco-R | 0-1289 | 28.75" | 28.0" | 0.803 |
| 24" | 186 | X-56 | RL 4S | 0-3680 | 22.5" | 22.25" | 0.497 |
| | 171.3 | | | 3680-6133 | | | |
| 18 5/8" | 136 | C-95 | TENARIS-ER | 0-9390 | 17.239" | 17.052" | 0.288 |
| 13 ½" | 81.4 | SS-110 | NK3SB | 0-13315 | 12.34 | 12.25 | 0.148 |
| 10 ¾" | 73.2 (Tieback) | SS-110 | NKHWC | 0-13000' | 9.406" | 9.25" | 0.0859 |
| | 73.2 (liner) | SS-110 | NKHWC | 13000-14226 | 9.406" | 9.25" | 0.0859 |
| 7-5/8" (Prod. Casing) | 55.3 (liner) | SS-110 | TNHWC | 13880-14723 | 5.875" | 5.7 | 0.0335 |
| | 55.3 (tieback) | SS-110 & T-95 | ADNJO & TNHWC | 0-9486 13880 | 5.875" | 5.7 | 0.0335 |
| 5" (Prodn. liner) | 21.4 | Q-125 | Hyd 513 | 14494-16473 | 4.126 | 4.001 | 0.0165 |
| 3-1/2" (Tbg.) | 12.95 | L-80 | Hydril 533 | | 2.75 | 2.625 | 0.00735 |

**Formations Tops & Temp**

| Formation | MD | TVD | Exp. BHT |
|---|---|---|---|
| Gotnia | | | |
| Najmah | 14222' | 14044' | |
| Sargelu | 14349' | 14162' | |
| Dharuma | 14449' | 14253' | |
| upper Marrat | 14573' | 14380' | |
| Middle Marrat | 14920' | 14685' | |
| Lower Marrat | 15630' | 15349' | |
| Minjur | 16358' | 16003' | |

| EST Pore Pr. (Drlg.) |
|---|
| 16.8 PPG @14723 ft |
| 15.4 PPG @15330 ft |
| 15.3 PPG @15703 ft |
| Max. 15.0 PPG @16467 ft |

| Radio Active marker | |
|---|---|
| Casing (in) | Depth (ft) |
| 7-5/8" | 14,223' |
| 5"(Liner) | 14,777' |

Formation: Middle Marrat
2-7/8" TCP, 6spf gun with Millenium charges
Interval:

Figure 1.5 Well Schematics and Casing Data.

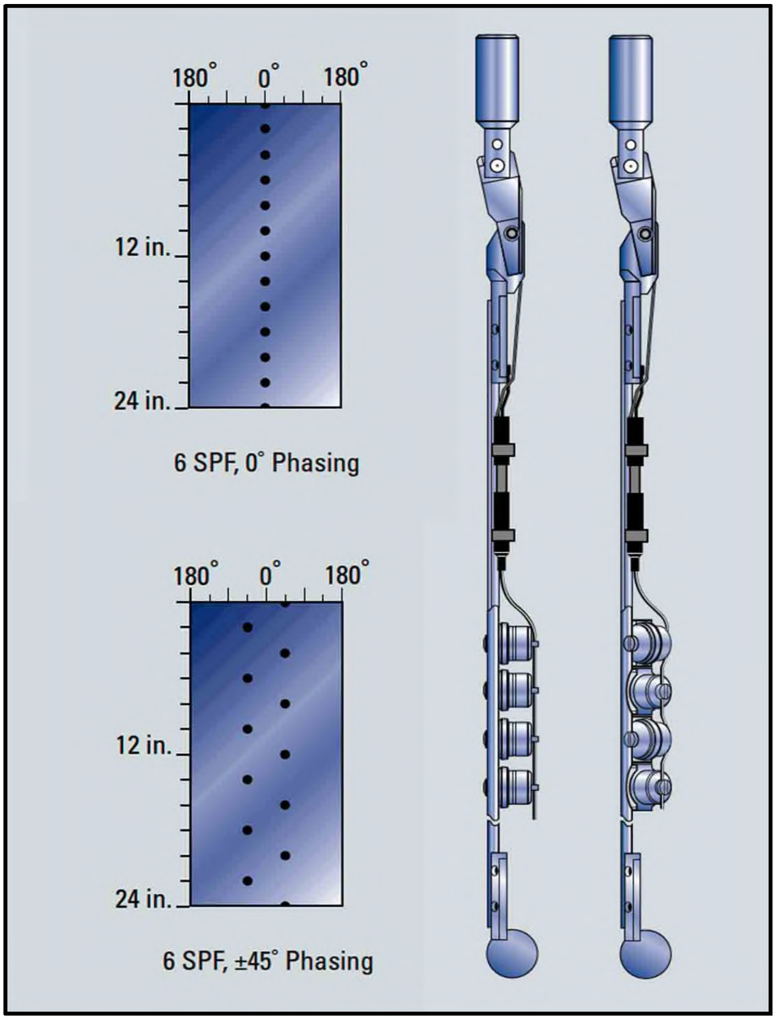


Figure 1.6 Gun Systems and Shot Patterns (www.slb.com).

The well logs in Figure 1.7 show good cement isolation with few natural fractures across the perforated interval. The porosity and permeability ranges are (5 – 18 %) and (0.1 – 10 mD) respectively, the distribution of these ranges is transformed in the reservoir model as demonstrated in Figures 1.8 and 1.9. The core lab tests observed the development of good porous reservoir facies. The seismic section interpretation denies the intersection of the well with any nearby faults.

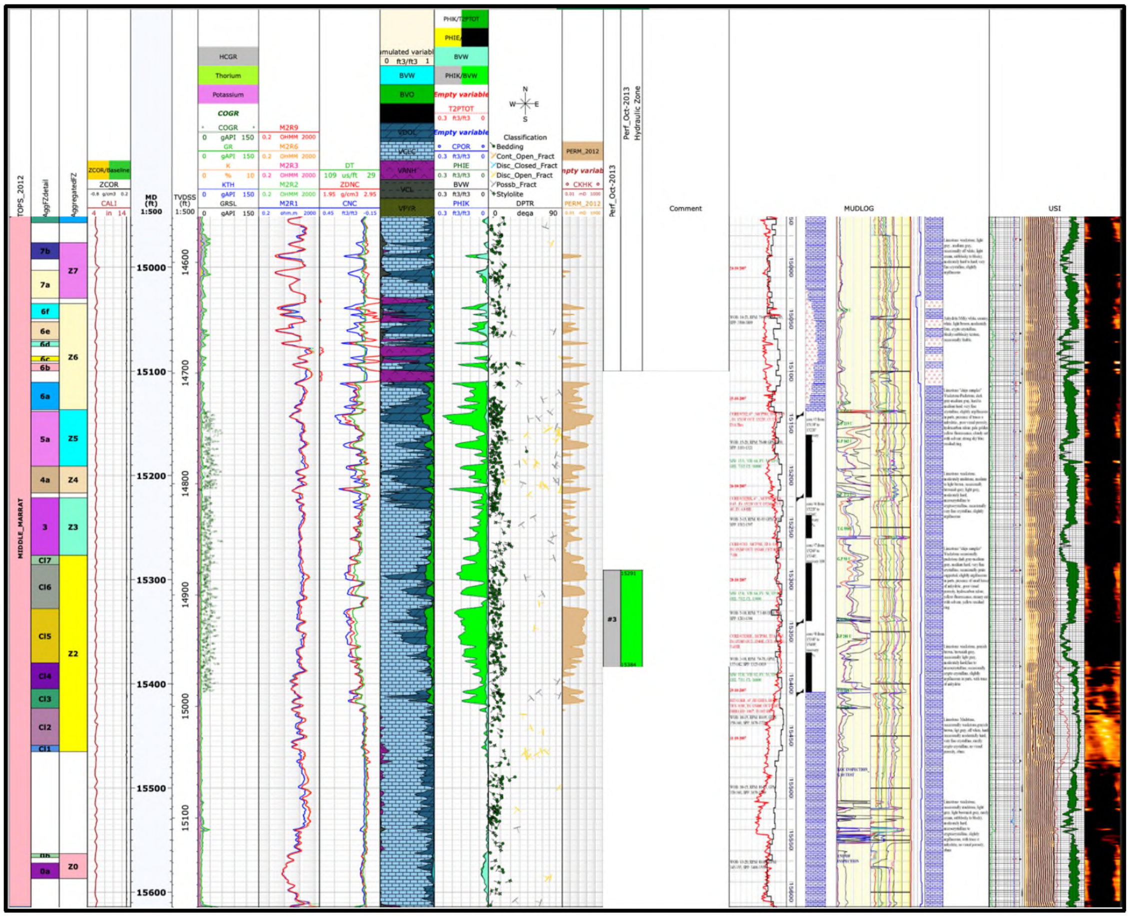


Figure 1.7 Composite Logs of Well MA-021.

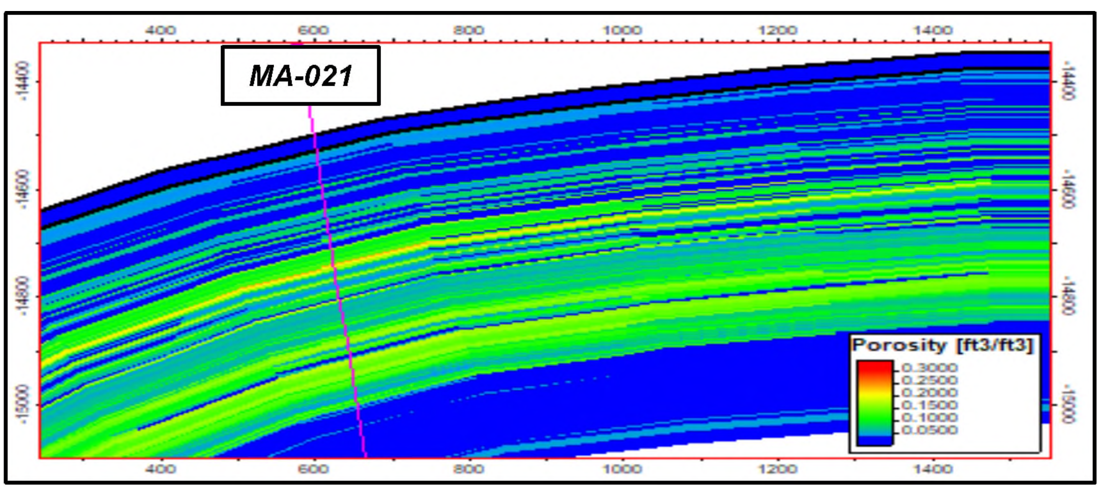


Figure 1.8 Well Cross-Section with the Distribution of Porosity Ranges.

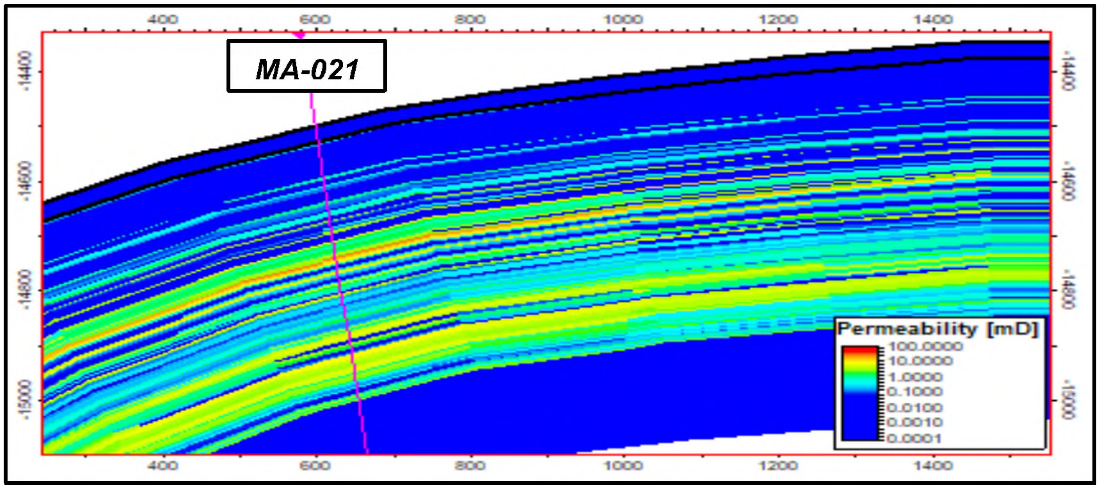


Figure 1.9 Well Cross-Section with the Distribution of Permeability Ranges.

The well was producing during a short-term test on 32”/64” choke size for 8 hours. The produced fluid had an API of 45 degrees with zero water production. A production logging tool (PLT) test was performed to identify the contribution from the perforated interval. It was found that most of the production is flowing from the upper part of the perforation interval as indicated in Table 1.2. The test also revealed that the actual perforation interval is shifted (- 36 ft) from the originally proposed perforation as illustrated in Figure 1.10.

Table 1.2 PLT’s Production Contribution Percentage.

| Production % | Zones ft |
|---|---|
| 39.83 | 15292.0-15307.2 |
| 8.49 | 15308.0-15324.3 |
| 27.12 | 15325.9-15350.9 |
| 21.17 | 15351.4-15364.4 |
| 3.39 | 15382.5-15385.0 |

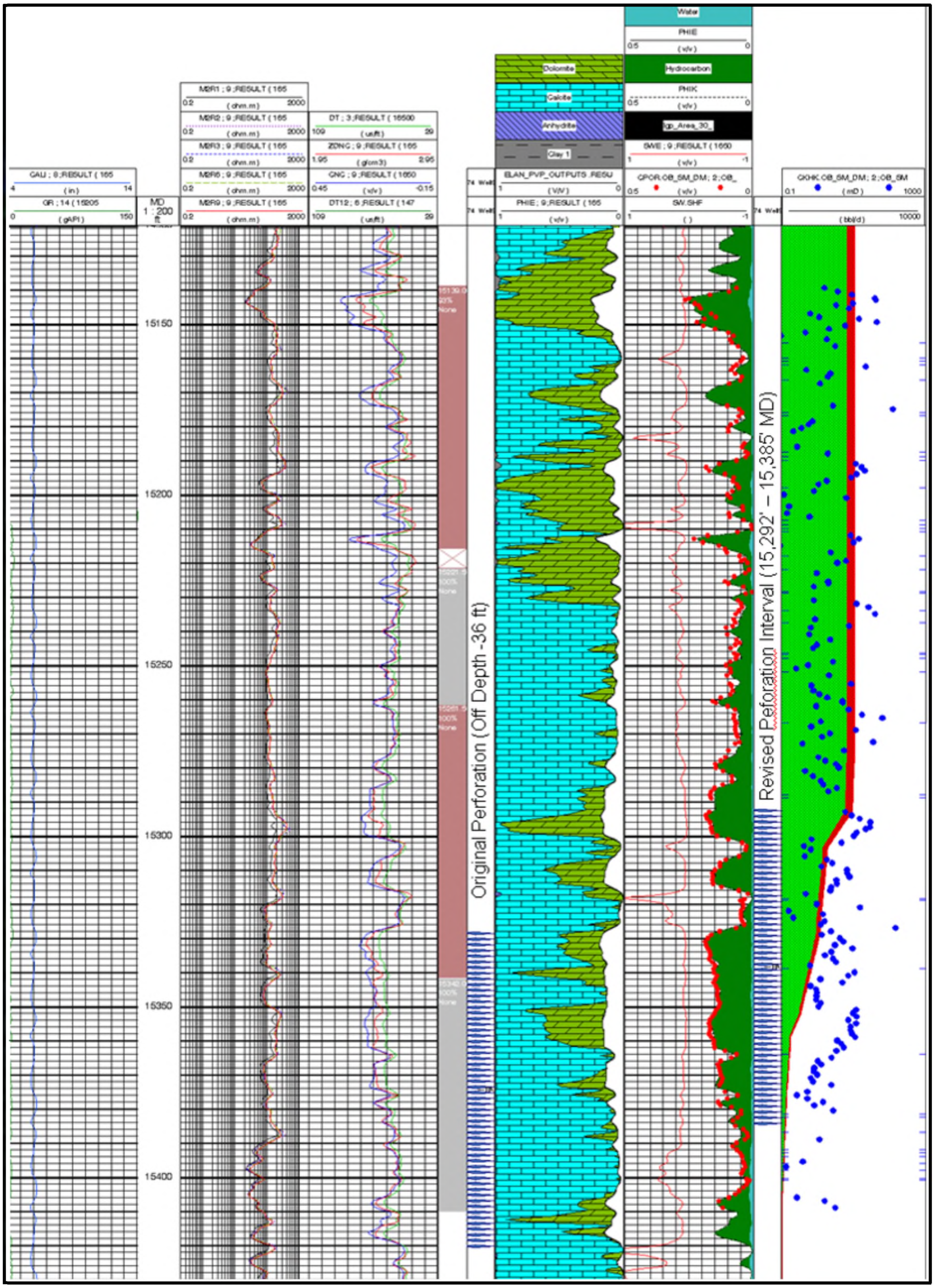


Figure 1.10 PLT Log Results.

## 1.2. OBJECTIVES

Before getting to the reasons behind this study, let us briefly discuss the behavior of wells in carbonate fractured reservoirs. The production plateau from a fractured reservoir tends to decline rapidly in a short time, relatively based on the number of natural fractures available in the formation. The initial high production rates represent the flow of hydrocarbons from the fractures into the wellbore, then it declines when the matrix starts feeding the fractures. At this point in the process of developing the well, the team turns to acid well stimulation or hydraulic fracturing to enhance the production.

MA-021, our subject of study was chosen for an acid (20% HCL) fracture job after showing a decline in production. Unexpectedly upon testing, the well showed only a 30% improvement in post-job production. This surprising result was noticed in several other wells without knowing the cause of such a poor outcome.

The main objective of the workflow demonstrated in Figure 1.11 that shapes this research is to investigate the post-acid fracture production and the poor results exhibited by the well through:

- Performing a forensic audit on all the available well data to examine and review the planning, acquisition, and execution phases.
- Modeling the actual acid-stimulation fracturing job performed on the well using StimPlan software.
- Compare post-fracture data interpretation results from StimPlan to the service company results.
- Run reservoir simulation on the studied well with the fracture input data from StimPlan's new fracture designs for evaluation.

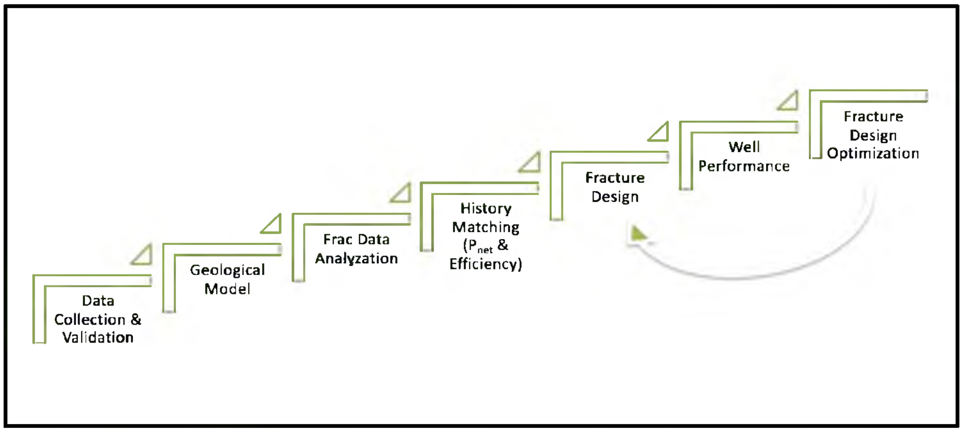


Figure 1.11 The Integrated Workflow of the Study.

## 1.3. LITERATURE REVIEW

The key factor for best stimulation results is to perfect the design of the fracture job. The outcome of the design can be simulated by lab experiments and numerical models creating workflows. These integrated workflows are used to calibrate the fracture design and optimize the results hence enhancing the recovery of the well.

For more than six decades, scientists and engineers in the oil and gas industry started to study and evaluate well stimulation process, trying their best to capture the controlling parameters behind it, to assist them in understanding the fracture propagation and conductivity which are critical in the process of their prediction.

The journey of studies and experiments started with a graphical estimation of productivity improvement using ratios of fracture conductivity to formation permeability, and fractured length to drainage radius as an estimation method for productivity improvement by McGuire and Sikora (1960). Followed by the analytical solution of utilizing fracture conductivity correlations to predict acid penetration length in the formation which was presented by Terrill (1965). Then a derivation of the productivity formula considering vertical fracture conductivity and radial steady-state flow was introduced by Raymond and Binder (1967). Sevougian et al. (1987) combined the productivity equation along with the conductivity correlations to estimate the optimum fracture length and conductivity for vertical wells. Ben-Naceur and Economides (1989) delivered guidelines addressing the importance of controlling the leak-off rate, avoiding fracture height, and maintaining width in the fracture design process. The numerical type curves were introduced to estimate productivity in low permeability reservoirs by Wattenbarger et al. (1998). A few years ago, Ravikumar et al. (2015) proposed fracture design procedures to estimate uniform fracture conductivity and optimum fracture length in acid-stimulated wells.

With the expansion and growth of computational power, researches and studies upgraded from lab experiments to the use of numerical models. These models have the ability to capture to some extent the interaction between the rock and the injected acid deep down in the reservoirs. Despite the existence of such a powerful tool, the degree of complexity created by the number of uncertainties and unknowns indicated in Figure 1.12 are so massive to be accounted for in a small number of models. It is very difficult even for us humans to keep track of all parameters and changes at the same time, as most of the features that affect the rock response to engineering activities remain hidden. In my personal opinion, the only possible way to integrate all of the required models at once is by using Artificial Intelligence (AI) as illustrated in Figure 1.13.

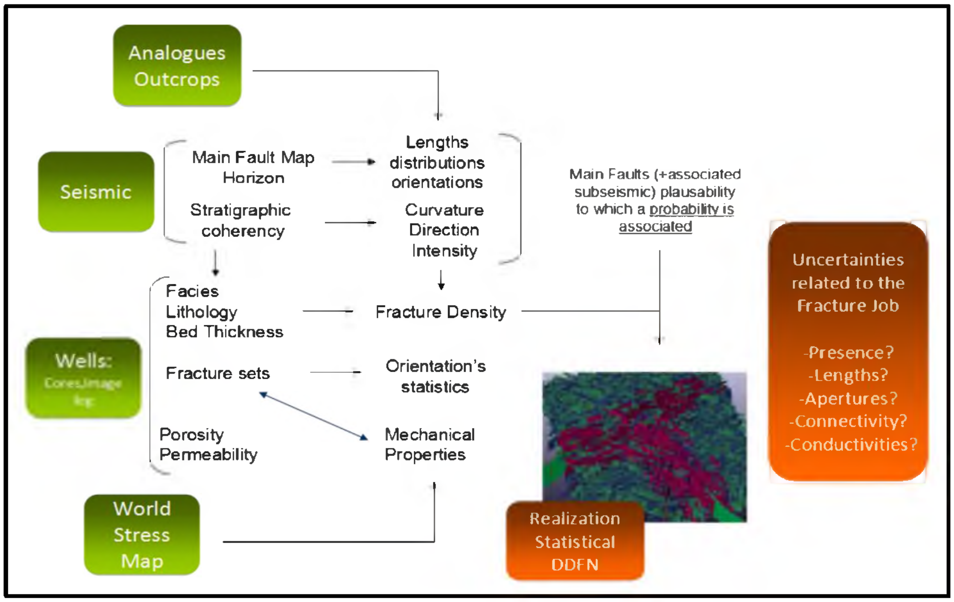


Figure 1.12 Some of the Fractures Associated Uncertainties (Delorme et al., 2014).

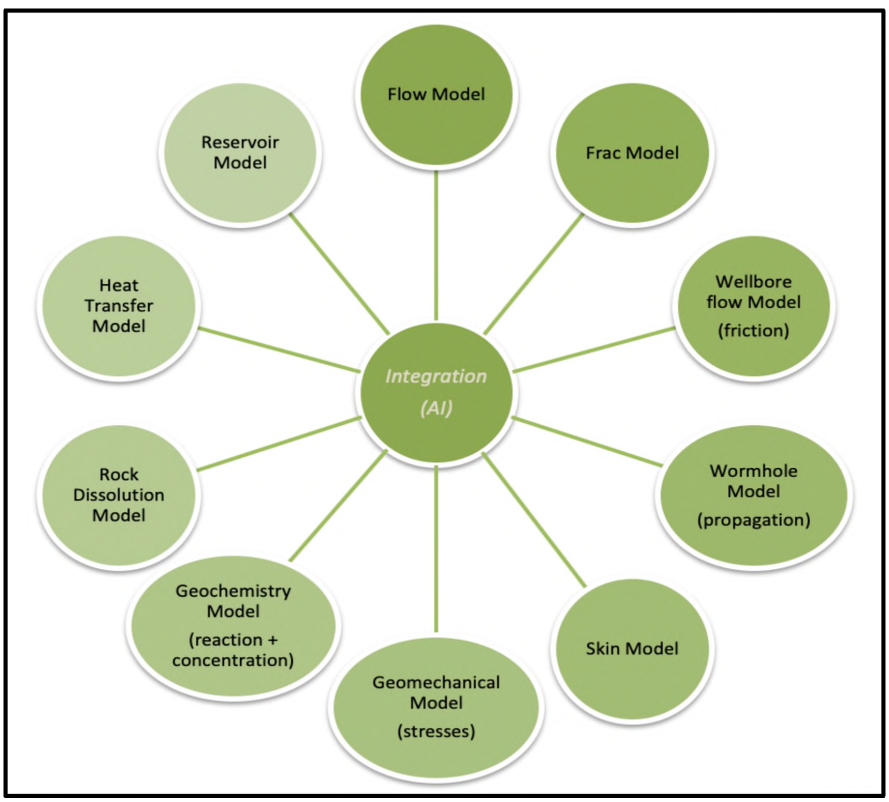


Figure 1.13 Types of Models used in Fracture Design Studies.

The mixture of fracture modeling and reservoir simulations creates a very powerful tool in field development, especially in unconventional studies. It has the capability of integrating production data, geological properties through the whole field minimizing the uncertainties in the undrilled areas between the wells, and performing multiple sensitivity studies. In addition to optimizing fracture designs, well completion, infill drilling, and re-fracturing. Allowing the engineers to integrate all of the available data to visualize the whole picture for better decisions making (Du et al., 2015; Tavassoli et al., 2013a, 2013b). It is famously known in the geological community, small evidence on the surface (logs and core) might be hard to extend to the deepest parts of the reservoir but definitely could guide us to better interpretations (Wennberg et al., 2009). That reminds me of one of Charles Lyell's principles of geology: "The present is the key to the past".

There are several studies on the subject of acid fracturing that helped in shaping the idea of this research. The majority of those studies include in their integrated workflow a fracture propagation model to generate the fracture, acid fracturing model to simulate the etching and fracture conductivity, and well performance model (Deng et al., 2011; Lo & Dean, 1989; Mou et al., 2010; Oeth et al., 2013; Oeth et al., 2011; Settari, 1993). Despite the fact that numerical models use estimated data and simplified assumptions to overcome the complexity, but still they are better solutions than the simple and fast classical approaches, which lack detailed results and most importantly the capability to generalize the results up to a full field scale (Delorme et al., 2016).

Jeon et al. (2016) presented a magnificent comparison between acid fracturing and fracturing with proppant shown in Tables 1.3, 1.4, and 1.5. Although the study outcome contradicts with the decision made on our subject of study, where they used acid to fracture the formation, there are many more reasons (economic conditions, cost of treatment, and cost of oil and gas) as stated by the authors which should be covered to be able to give a proper decision. As we all know, operational cost plays a strong role in the decision-making process in the industry, because it affects the profit thus affecting the success of the entire project.

Table 1.3 Strengths of Proppant and Acid Fracturing (Jeon et al., 2016).

| Proppant Fracturing | Acid Fracturing |
|---|---|
| • Fluids are not reactive and corrosive to downhole tubulars.<br>• Fracture dimensions can be determined by proppant addition and distribution.<br>• High strength proppant commonly ensures better fracture conductivity in deep wells.<br>• Longer fracture length can be achieved in tighter formations by increasing total fracturing fluid volume pumped.<br>• Leak-off is not significant problem as it can be easily controlled with available additives. | • It has simpler process than Proppant fracturing.<br>• It it highly applicable in high permeable reservoirs as acid dissolves formation and enlarges flow channels while etching.<br>• Wellhead pressure is usually not restricted.<br>• Conceptually it can have higher fracture conductivity; unless limited by severe reservoir conditions, very high fracture conducvity can be achived.<br>• Since it does not require flush stage, fast well clean-up and ready-well-reponse is attainable.<br>• There is no screen-out concerns. |

Table 1.4 Limitations of Proppant and Acid Fracturing (Jeon et al., 2016).

| Proppant Fracturing | Acid Fracturing |
|---|---|
| • Higher operation cost is expected due to large volume of padding fluid and proppants.<br>• Proppant usage brings a concern of placement in the fracture and screen-out to formation.<br>• In high deliverability wells, proppant flow back may occur.<br>• It is expensive to clean out the wells once screen-out happens.<br>• Soft carbonates under high closure stress often experiences proppant embedment problem even though it can be remedied with wider propped fracture design. | • Due to acid reaction with formation, high fluid leak-off is problematic.<br>• Acid reaction does not allow long etched fractures.<br>• Corrosion inhibitors are always required to protect the treatment facilities.<br>• Strategic acid placement is required to obtain stable fracture conductivity at high effective pressures.<br>• Deep, high temperature wells commonly require more expensive organic/HCl blends.<br>• Soft carbonates under high effective stress can re-heal. |

Table 1.5 Treatment Recommendation Based on Simulation (Jeon et al., 2016).

| Serial # | Case Name | Best option for fracturing | | |
|---|---|---|---|---|
| 1 | Deep reservoir | Acid frac | High strength proppant | Low strength proppant |
| 2 | Shallow reservoir | Acid frac | High strength proppant | Low strength proppant |
| 3 | High pore pressure | Acid frac | High strength proppant | Low strength proppant |
| 4 | Low permeability | Acid frac | High strength proppant | Low strength proppant |
| 5 | High porosity | Acid frac | High strength proppant | Low strength proppant |
| 6 | High Young's modulus | Acid frac | High strength proppant | Low strength proppant |
| 7 | High temperature | Acid frac | High strength proppant | Low strength proppant |

**1.3.1. KOC Study.** The aim of the study was to test three different unconventional approaches on one of Kuwait's tight carbonate reservoirs, to decide on the most optimum method to model stimulated fractures. These approaches are as follows:

- Well-bore PI multiplier.
- Matrix permeability multiplier (SPSP model).
- Dual-media model (DPDP model).

Sensitivity analysis was also performed to overcome the uncertainty with fracture permeability, as it was calculated using Poiseuille's law. The study concluded that the DPDP model produces the best results in modeling stimulated fractures (K. Tiwari et al., 2019). Therefore, in this study, a DPDP model is used in the reservoir model to enhance the outcome of implementing the fracture geometry and conductivity from the fracture model.

**1.3.2. Integrated Workflows.** The structure of the integrated workflow presented in this research was introduced and discussed in the literature within various studies. With the use of different data, approaches, methods, and ideas, studies can build on each other aiming at solving the targeted enigma.

The acid fracture research laboratory at Texas A&M University presented great studies delivering integrated workflows that helped in shaping this research's workflow. The first study was applied on a carbonate reservoir (100% limestone) with three models combined to produce a unique workflow, which enables the user to evaluate and optimize the fracture design (Wu et al., 2013). The generated models are:

- Fracture propagation model: for fracture geometry using StimPlan software.
- Acid transport and dissolution model: for the etched fracture conductivity in each cell using correlations.
- Well performance model: for well production rates using Eclipse software.

The second study introduced two-way modeling workflows; the normal forward integrated workflow and inversion integrated workflow, which aimed to overcome unavailable input data (leak-off coefficient) (Jin et al., 2017). The used models are:

- Fracture propagation model: for fracture geometry using Mfrac software.
- 3D fracturing model: for fracture conductivity in each cell using correlations.
- Well performance model: for well production history match using Vogel inflow performance model.

In the third study, they used integrated models coupled with a reservoir model for optimum stimulation design, with the use of fracture conductivity distribution along the created fracture. It is worthy of note that the fracture geometry and conductivity were simulated during the injection and closure periods, meaning that the values are not constant (Aljawad et al., 2018). The models constructed the workflow are:

- Acid fracture models:
    - Fracture propagation model (fracture geometry).
    - Acid transport and reaction model (acid).
    - Heat transfer model (temperature).
- Productivity model: for productivity index calculations.

This last study contained a unique way of constructing the workflow. Using a data-rich well as a subject of study enabled in producing a fully integrated fracture treatment evaluation. The detailed reservoir characterization data linked with the models boosted the capability of evaluating and optimizing fracture treatment designs (Offenberger et al., 2013). The list of the models is as follows:

- Geo-cellular model.
- Discrete fracture network model (DFN).
- Reservoir model: PVT data, permeability, relative permeabilities, porosity, and saturations.

**1.3.3. Post-Stimulation Production.** Some several uncertainties and unknowns surround the well performance after the fracture job, including direct and indirect affecting factors. What makes it more complicated, is that the reasons differ from case to case. To fully investigate the matter, the whole process of stimulation needs to be monitored and reviewed, starting from the planning phase, passing through data collection, and finally the operation execution phase. Acid stimulation in carbonate reservoirs might cause wellbore damage, causing the change in skin factor resulting in getting smaller production rates than expected. Therefore, the estimation of skin factors before and after the fracture job is highly important, as it might be the cause of the underperformance of the well (Jin et al., 2017).

Any fracture engineer knows the importance of geomechanics for placing wells and designing the fracture job. Formation stresses can be another key factor affecting post-stimulation production. Etching the formation, especially near-wellbore may result in a change in stresses and in some cases collapse of the completion casing. Thus, an assessment of the mechanical damage on the acidized rock is critical to ensure long-term production (Safari et al., 2017).

**1.3.4. Induced and Natural Fractures.** The future of a certain field can be determined by the existence of natural fractures in the reservoir and the level of understanding of the interaction between those natural fractures and the induced ones (Delorme et al., 2016). Natural fractures can sometimes affect negatively on the conductivity of the created fracture, as they steal a fraction of the injected acid designed for the main fracture causing a reduction in the fracture conductivity (Ugursal et al., 2019). In addition to that, in some cases, the natural fractures orientation is perpendicular to the induced fracture. This system of alignment causes the induced fracture to propagate in the same direction as the naturally existing fractures negating their effect on improving the production (Li et al., 2012).

# 2. METHODOLOGY

## 2.1. DATA COLLECTION AND VALIDATION

Data availability can push the project drastically to the point of success. That's why this first step of the study is extremely important, it is the base rock that will hold the rest of the research. Before collecting the data, a review of over 70 wells from six different fields took place to select the candidate well for the study. The criteria of selection were based on data availability, reservoir, and areas with the least simulation problems and errors in the model. Two wells were selected, MA-021 our primary selection and another well used as a backup.

During the validation process of the collected data shown in the background section, it was found that the well trajectory wasn't correctly represented, as the well was vertical in the model while it is actually deviated. That dates back to the time at the beginning of the project when the team used simple methods (Microsoft Excel software) to draw the schematic of the well to save time because in the early stages contracting with software companies process takes time. Keeping a small note in the corner of the schematic wasn't enough to avoid this error.

Moreover, the shift in the perforation interval discovered in PLT was not modified in the well data in the reservoir model. Lastly, the latest tubing check performed in the well revealed with the help of an impression plug, that there was a wire left in the hole during one of the jobs. Which can cause blockage, formation damage, and corrosion in the long term.

Another part of the validation was to review the fracture job proposal. This proposal is a document provided by the service company that will handle the execution of the fracture job. The document provides information on the fracture design in terms of; lab tests, type of treatment, job schedule, and procedures. Most of the information delivered in the proposal was produced from fracture model simulations. One of these simulations, mimics the fracture in the formation, providing height, width, and conductivity of the fracture as illustrated in Figure 2.1.

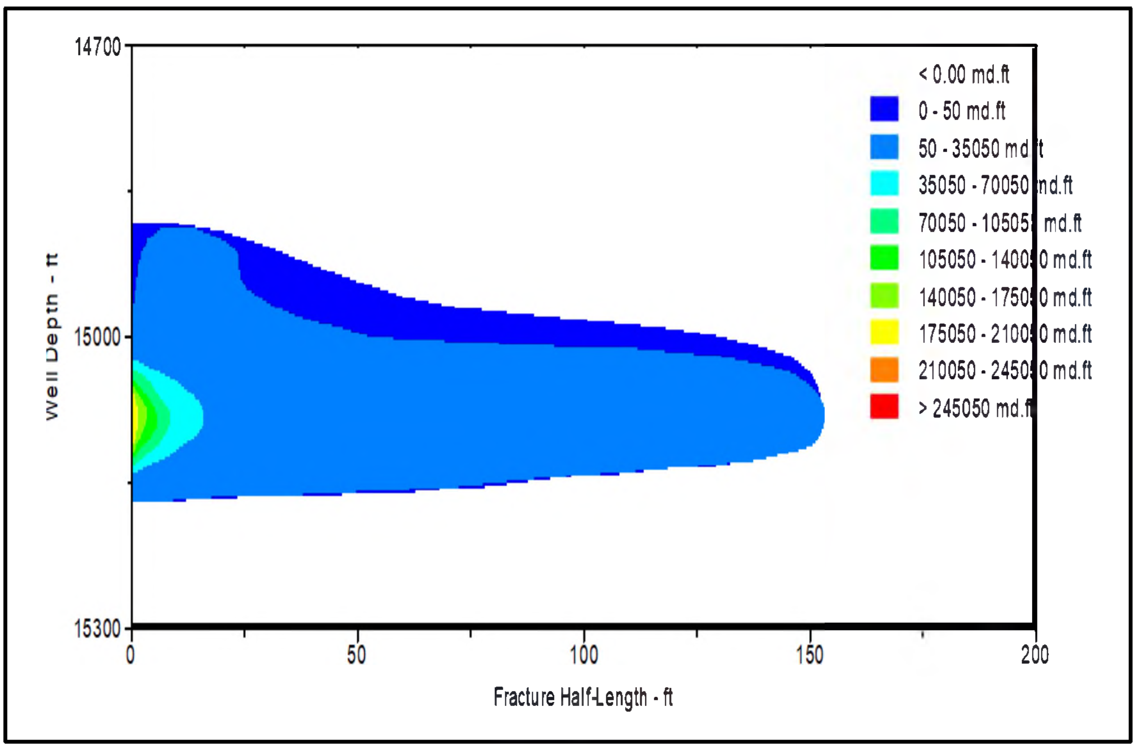


Figure 2.1 Simulated Fracture Length and Conductivity.

The simulated fracture shows around 280 ft of fracture height and about 150 ft of fracture length, which is not bad if it is the actual fracture results. Nevertheless, it is not necessary for the actual induced fracture to be identical to the simulated one, since the shape of the final induced fracture is controlled by the results of the mini fracture tests performed before the main fracture. The issue with the service company's proposal results is that the simulated fracture does not intersect with either the old perforations (15328 – 15421 ft) or the new revised one (15292 – 15385 ft).

## 2.2. FRACTURE MODELING

The fracture modeling part was performed with the use of StimPlan software, one of few fracture modeling software available that have the capability of fully 3D fracture modeling. The software also has the feature of acid stimulation (acidizing), which will enable us to mimic the actual fracture job and analyze the results. The software was introduced to the industry by NSI Technologies Company in the mid-'90s. The main purpose of the fracture modeling part is to obtain the fracture input parameters for the reservoir simulator. Those parameters are fracture geometry and conductivity, with which we can evaluate and optimize the fracture design. The software has a variety of plots that work as tools of interpretation and analysis on both real-time and recorded data from the executed fracture job. It also gives the user the ability to design the fracture treatment and test it by simulating the fracture geometry and proppant distribution.

**2.2.1. Geological Model.** The first step was to structure the geological model in StimPlan by using actual field data. The logging process in the Jurassic wells usually covers only the zone of interest, but luckily in MA-021, Raw log data covers the whole unconventional reservoirs, starting with the top of Najma-Sargelu and ending with the base of the Middle Marrat reservoir. This thickness will enable us to test fracture designs with less worry of breaking through the formation boundaries. Feeding the software with reservoir data (pressure and gradients) enables it to calculate the static and dynamic Young's modulus and Poisson's ratio of the formation as demonstrated in Figure 2.2.

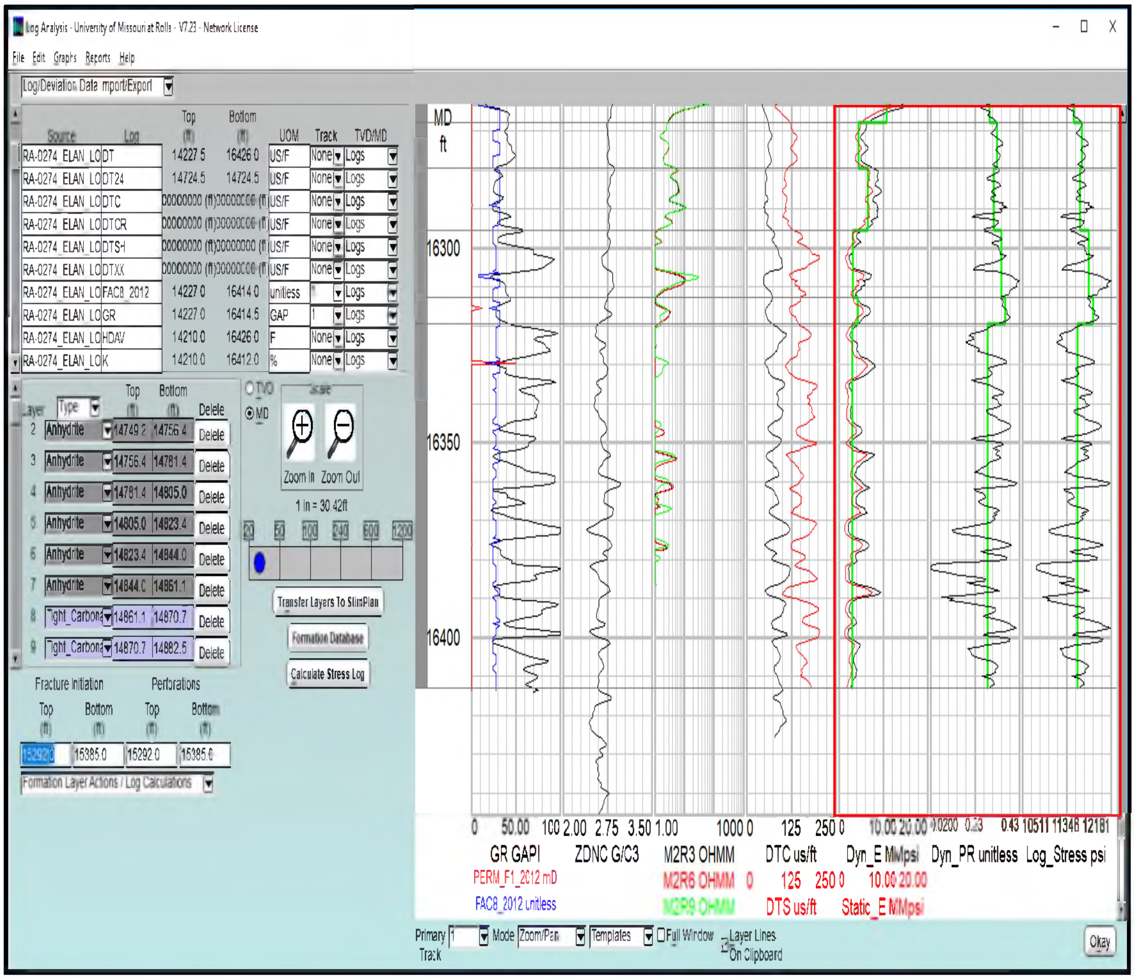


Figure 2.2 Imported Well Logs and the Calculated Data.

The calculated logs need to be averaged to smooth the curves and for better integration as a preparation for the layering process. The maximum layer number allowed in the software is 100, which has a direct effect on the simulation run time. Therefore, two sets of models were built, a main 80 layers primary model, and a smaller 40 layers model in case the simulation run was consuming a long time. The changes in gamma-ray, Poisson's ratio, Young's modulus, and stresses drive the layering process. In the primary model, three rock types were assigned to the layers based on permeability and facies logs as indicated in Figure 2.3. The types of rocks are:

- Anhydrite: seal (black).
- Dolomite: porous (blue).
- Tight carbonate: low porosity (purple).

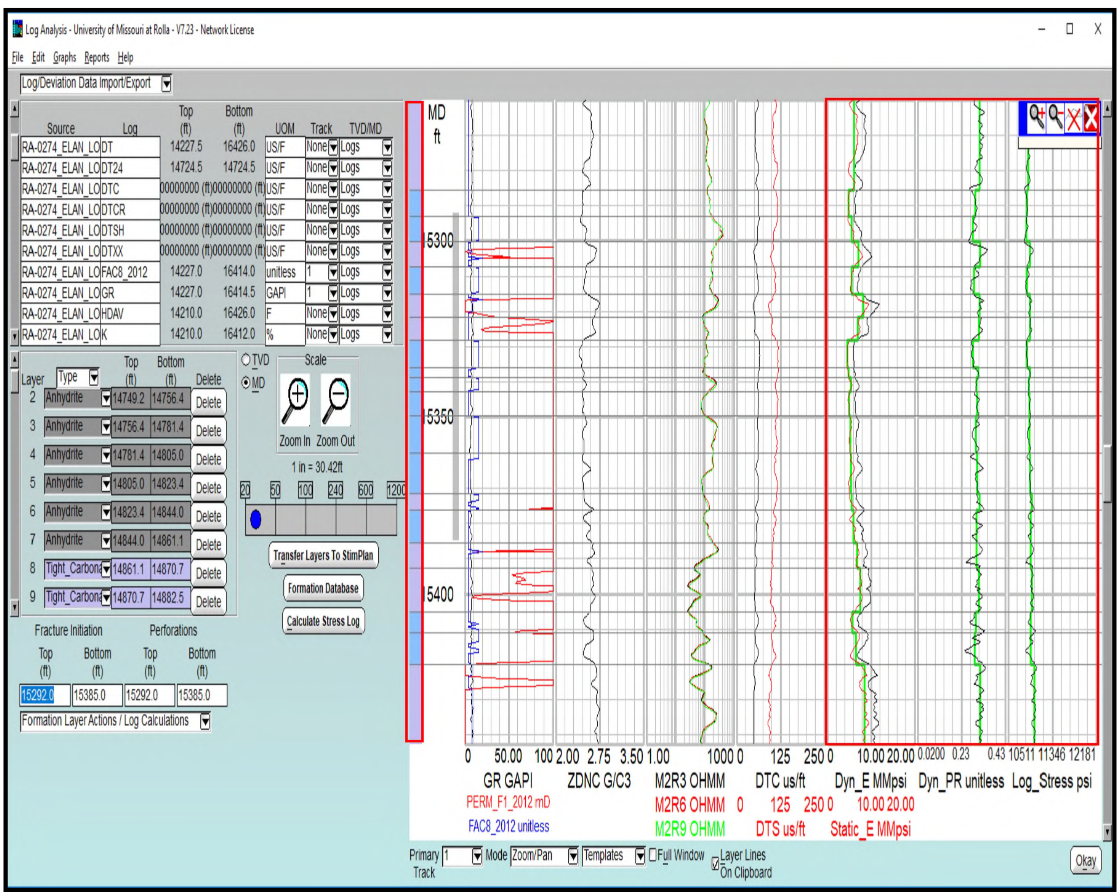


Figure 2.3 Averaged Logs with the Assigned Rock Types.

**2.2.2. Post-Fracture Data Analysis.** The pressures, pumping rates, time, and volumes that ought to be analyzed in StimPlan are actual data gathered and recorded from separate tests in the fracture job. In the field, they are sometimes called mini fracs. In MA-021, the fracture tests performed are:

- Injectivity test: pumping a volume of slickwater to create the initial break in the formation and obtain the fracture data.
- Step rate test: to test the response of the formation with different pumping rates by slickwater as the pumping fluid.
- Calibration test: a mini fracture with small volume to test the response of the formation with the actual treatment fluid (ClearFrac).
- Main fracture: pumping the treatment volumes as designed for the main fracture job.

Every test has its data that have to be imported separately in the software. The periods of injection and decline for each test has to be specified individually for plotting as shown in Figures 2.4, 2.5, and 2.6.

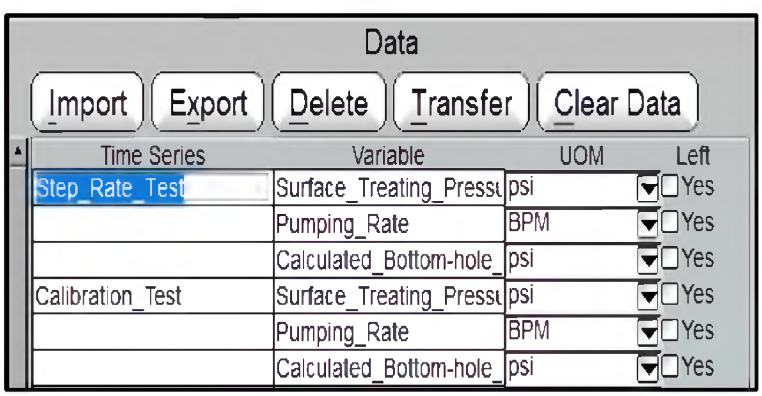


Figure 2.4 The Imported Fracture Data from Field Tests.

| Test | Start Time | End Time | Analyze |
|---|---|---|---|
| SRT_Decline | 19.30 | 52.31 | Go |
| SRT | 0.00 | 19.30 | Go |
| SRT_Step-Down | 14.50 | 19.60 | Go |
| Calibration_Injection | 1.90 | 20.10 | Go |
| Calibration_Decline | 20.10 | 81.62 | Go |

Figure 2.5 Data Classification Based on Injection and Decline Periods.

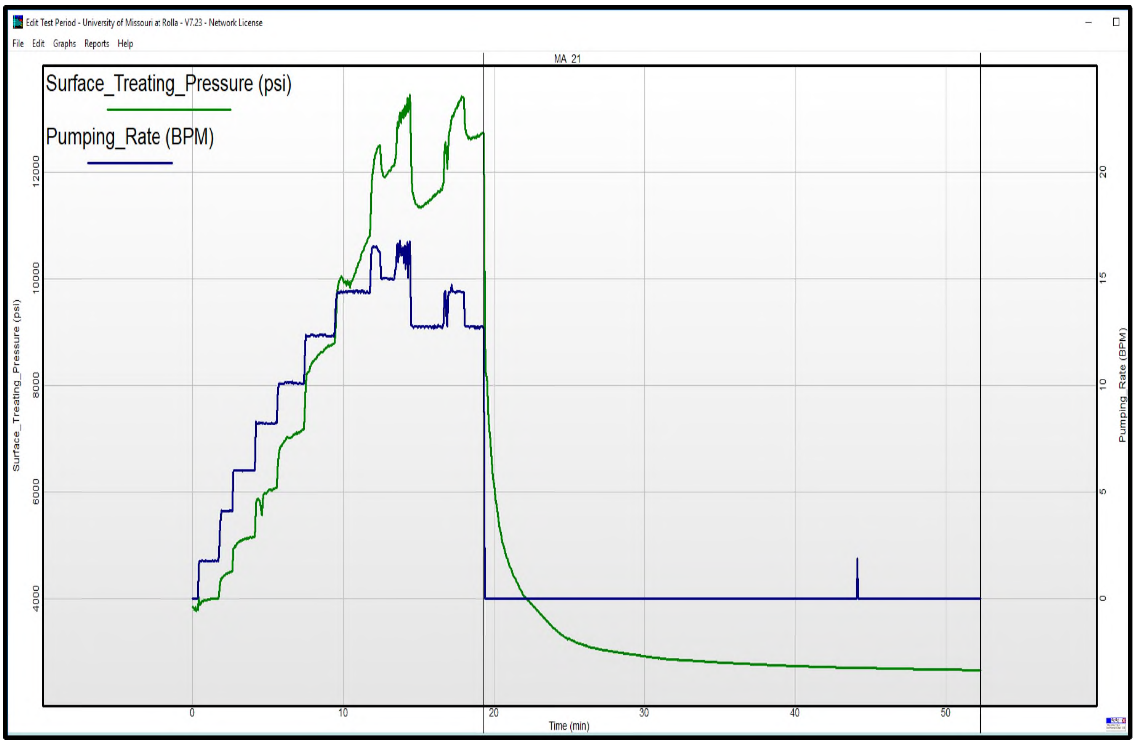


Figure 2.6 Decline Period on the Treatment Plot.

StimPlan offers several plots used as tools of analysis and interpretation, which ease the process and provide better results and consistency as illustrated in Figure 2.7. The plots types are:

- Horner plot.

- ISIP plot.
- Log-log plot.
- Bourdet plot.
- Square-root of time plot.
- G-function plot.
- Barre plot.

The closure pressure, ISIP, and fluid efficiency from each plot should be consistent and in agreement with one another. This consistency in the interpreted data will impact the history matching process in StimPlan positively and reduce the time needed for the match. The best results of fluid efficiency and net pressure were transferred to the structured geological model in StimPlan as preparation for history matching.

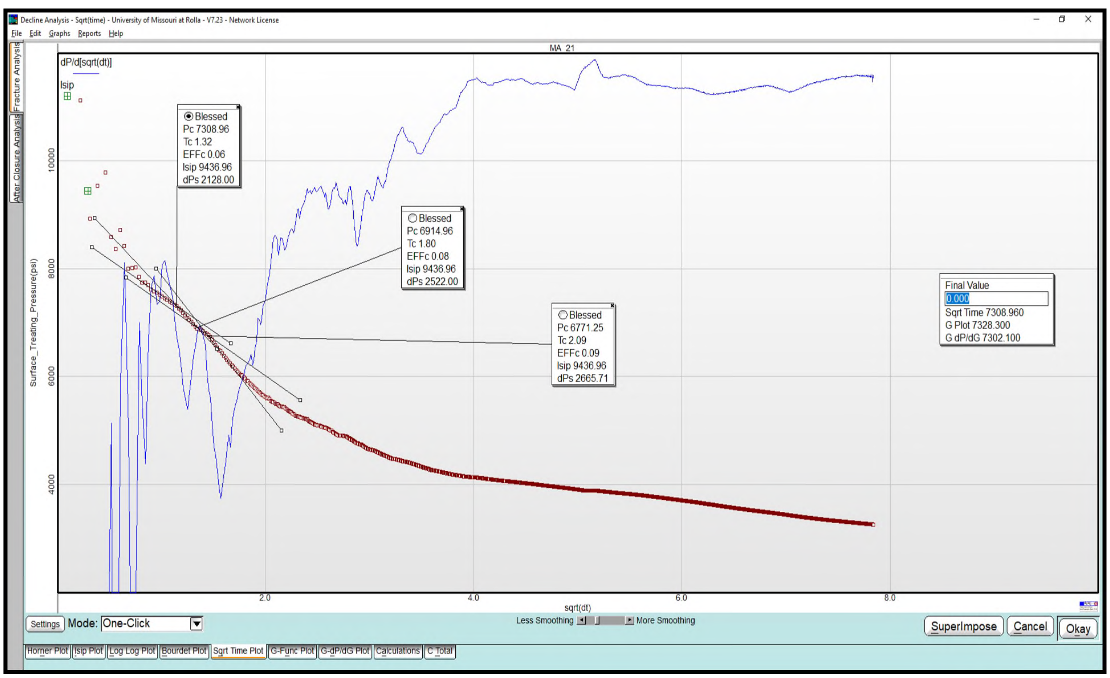

Figure 2.7 Data Interpretation via the Square-Root of Time Plot.

**2.2.3. History Matching.** The constructed geological model was calibrated by history matching the net pressure data and fluid efficiency. The tuning parameters in this process are the formation's leak-off coefficient and the stress contrast between the previously assigned layers in the model. In Figures 2.8 and 2.9, the simulated fluid efficiency should match the one measured in the fracture job, and the simulated net pressure must overlay the measured data in the plot.

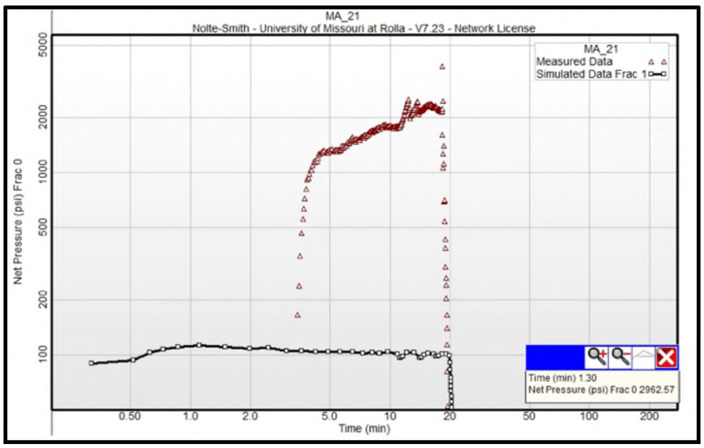


Figure 2.8 Unmatched Net Pressure Data.

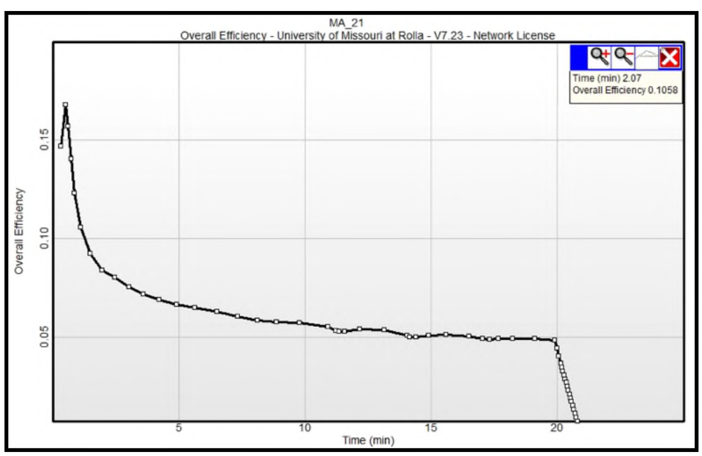


Figure 2.9 Unmatched Fluid Efficiency Data.

The fluid properties in StimPlan should represent the one that was used in the fracture job. Therefore, the service company was contacted to request the fluid data in Table 2.1, and they faced a hard time locating the data since it was from more than 10 years ago.

Table 2.1 Fluid Properties used in the Fracture Job.

| Shear Ramp | Cycle No | Time (min) | Temperature (°F) | n' | Kv (lbf-s^n /100 ft2) | Coef. Detn.(R^2) | K'(lbf-s^n /100 ft2) | K' slot(lbf-s^n /100 ft2) | Visc@ 40(1/s)(cP) | Visc@ 100(1/s)(cP) | Visc@ 170(1/s)(cP) |
|---|---|---|---|---|---|---|---|---|---|---|---|
| 1 | 1 | 35.1 | 248 | 0.31756 | 6.488818 | 0.9911 | 5.947415 | 7.060389 | 272.69 | 145.92 | 101.59 |
| 1 | 2 | 65.1 | 254 | 0.37176 | 5.026809 | 0.971 | 4.635022 | 5.47254 | 258.15 | 145.17 | 104.01 |
| 1 | 3 | 95.1 | 255 | 0.39605 | 4.458223 | 0.9629 | 4.12232 | 4.851021 | 250.28 | 143.91 | 104.45 |
| 1 | 4 | 125.1 | 255 | 0.40925 | 4.18124 | 0.9631 | 3.872221 | 4.547572 | 246.33 | 143.36 | 104.78 |
| 1 | 5 | 155.1 | 255 | 0.41593 | 4.048848 | 0.966 | 3.752589 | 4.402381 | 244.41 | 143.12 | 104.98 |
| 1 | 6 | 185.2 | 255 | 0.41902 | 3.992593 | 0.9693 | 3.701811 | 4.340627 | 243.74 | 143.13 | 105.16 |
| 1 | 7 | 215.1 | 255 | 0.41916 | 3.996325 | 0.9719 | 3.705336 | 4.344655 | 244.1 | 143.36 | 105.34 |

The history match was performed on two models; 1D model and 3D model. Although using the 3D model consumed greater time, it was needed to test the effect of adding 20% HCL to the fracture fluid on the results, which is a feature only available in the 3D model.

**2.2.4. New Fracture Designs.** The last part of the fracture modeling section is the creation of fracture designs, to be evaluated with the reservoir simulator. Four fracture designs were generated and simulated in both 1D and 3D models based on the treatment total volume (2000 BBLS) used in the fracture job. The software simulates the provided designs and illustrates the fracture geometry with the distribution of the proppants inside as demonstrated in Figure 2.10. A detailed report can also be produced for the results of the simulated design as shown in Table 2.2. The designs are classified and described as follows:

- Frac_design_slb: this design was an attempt to recreate the service company's design by providing StimPlan with the desired fracture half-length as illustrated in Figure 2.11.
- Frac_design_01: to test the outcome of almost the same pumping schedule of the fracture job without the inclusion of proppant.
- Frac_design_02: the design was driven by the dimensionless fracture conductivity equation to obtain the optimum fracture design where $F_{cd}$ equals 2, with the inclusion of proppant.
- Frac_design_03: aims to test the effect of a multi-stage pumping schedule (pumping cycles).
- Frac_design_04: only applicable in the 3D model to solely test the effect of adding acid (20% HCL) to the fracture fluid.

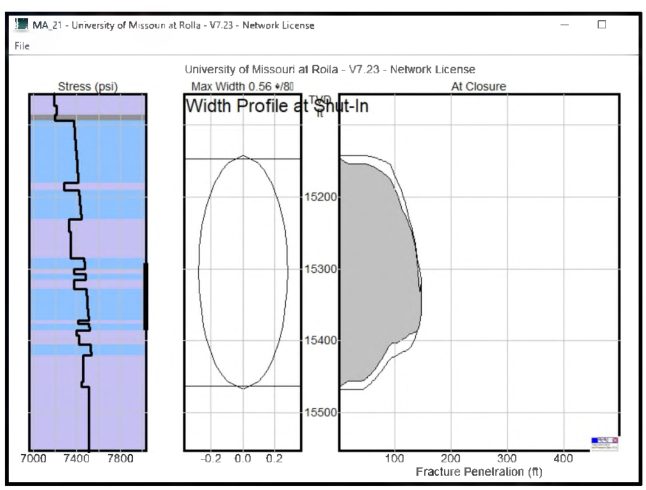


Figure 2.10 An Example of Fracture Geometry and Proppants Distribution.

Table 2.2 An Example of Calculated Results of the Design.

| Calculated Results | | |
|---|---|---|
| **from 3-D Simulator - StimPlan 1-D** | | |
| **Pumping Schedule - Frac_design_slb** | | |
| **Geologic Model - MA-21_M.Marrat_L80** | | |
| **Licensed To: University of Missouri at Rolla - V7.23 - Network License** | | |
| **Frac 1Perforations : 15292.00-15385.00 ft MD / 15292.00-15385.00 ft TVD** | | |
| Half Length | 'Hydraulic' Length (ft) | 148.0 |
| | Propped length (ft) | 144.7 |
| PRESSURE: | Max Net Pressure (psi) | 2476.8 |
| | Final Net Pressure (psi) | 1503.6 |
| | Maximum Surface Pressure (psi) | 2758.4 |
| TIME: | Max Exposure to Form. Temp. (min) | 0.4 |
| | Time to Close | 17.6 |
| RATE: | Fluid Loss Rate during pad (BPM) | 19.63 |
| EFFICIENCY: | At end of pumping schedule | 0.04 |
| PROPPANT: | Average In Situ Conc.(lb/ft^2) | 0.41 |
| | Average Conductivity (md-ft) | 173.7 |
| HEIGHT: | Max Fracture Height (ft) | 325.6 |
| WIDTH: | Avg width at end of pumping (in) | 0.31 |
| VOLUMES: | Total Fluid Volume (M-Gal) | 423.4 |
| | Total Proppant Volume (M-Lbs) | 25.6 |

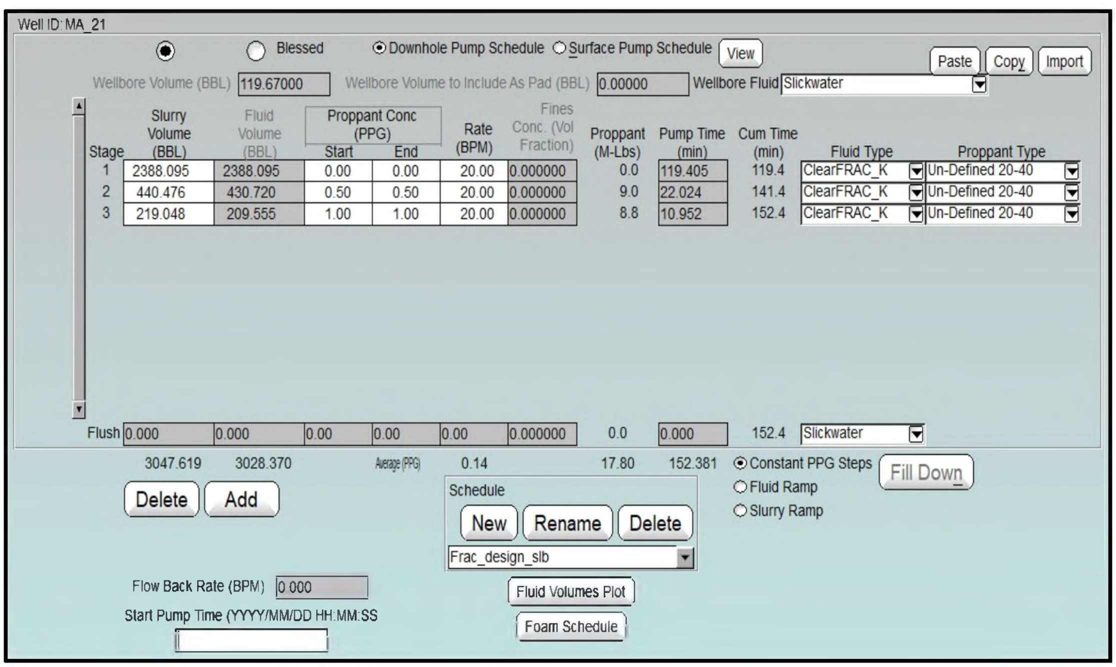


Figure 2.11 The Pumping Schedule of One of the Designs.

## 2.3. RESERVOIR SIMULATION

The role of reservoir simulation in this study is to evaluate the fracture designs by forecasting the well production performance. In this section, two software were used, Petrel as an interface for the reservoir model, and Eclipse as the engine or the numerical simulator. The power of these packages in field development might be a strong reason behind the decision of KOC to used them. In addition, the feature of hydraulic fracturing and the ability to capture the effect of fracture geometry and conductivity in the well was the main reason for our selection. The model has a DFN that captures the existence of natural fractures in the formation, which will to some degree covers their effect on the forecasted post-production. The software also adapts a DPDP model, that will simulate the fluid flow from the fractures to the wellbore and from the matrix to the wellbore through the fractures.

**2.3.1. Well Sector Model.** The static model was constructed at the beginning by integrating seismic data along with the data acquired from the drilled wells. The drilling plans helps in updating the model with new information obtained from the newly drilled wells every year. Tests on field fluid samples feed the model with the required data to simulate the fluid flow through the formation rocks. Both fluid properties and core lab test results are entered to bring the model to life, in other words, changing it from static to dynamic model. Additionally, the model helps in calculating and propagating data in the undrilled areas between the wells to overcome the unknowns and address part of the uncertainties. All these advantages explain the high cost of the modeling software packages, but in turn, it will save time, effort, and maximize the economic gain by allowing the user to take better and faster decisions.

The main model in Figure 2.12 was built to represent all six fields of the Jurassic project. The total area of the model was segregated into regions based on faults, pressures, contacts, and reservoir boundaries.

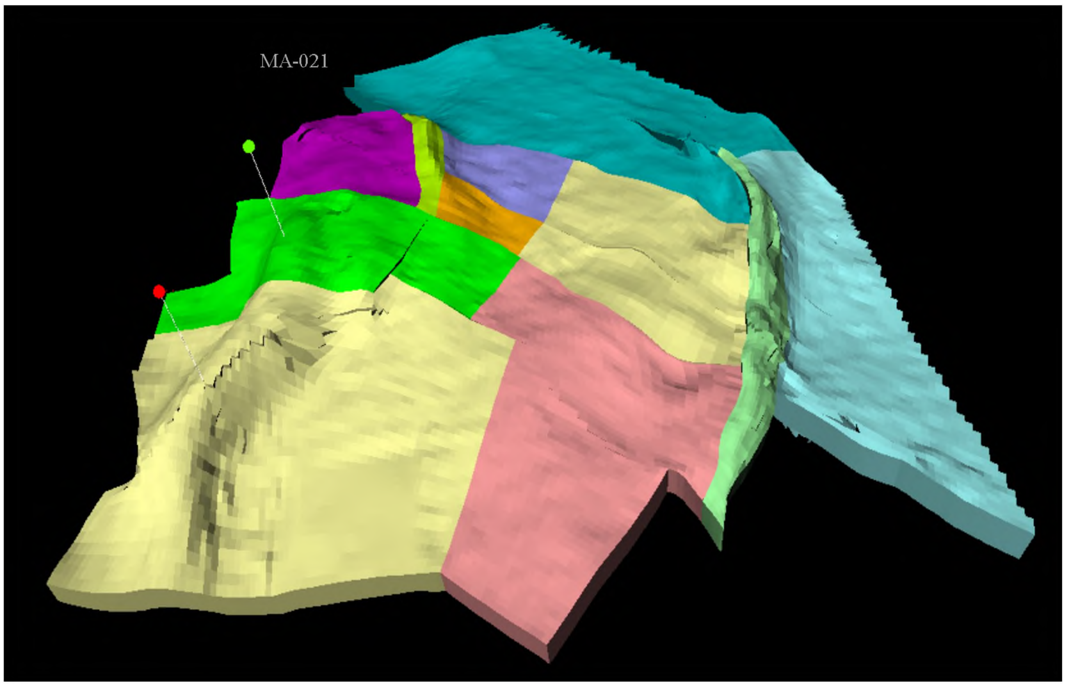


Figure 2.12 Full Model with Segregated Regions.

An 8 x 8 cells sector model was created with the use of distance from well properties shown in Figures 2.13 and 2.14. The idea was to contain the effect of induced fracture and its length within the boundaries of the sector model. This step was performed on both fine and upscaled models, where the simulation run time will be the judge on the one to use. A local grid refinement was implemented to give more detailed information around the wellbore, but the huge cell count indicated in Table 2.3 affected the simulation run time negatively.

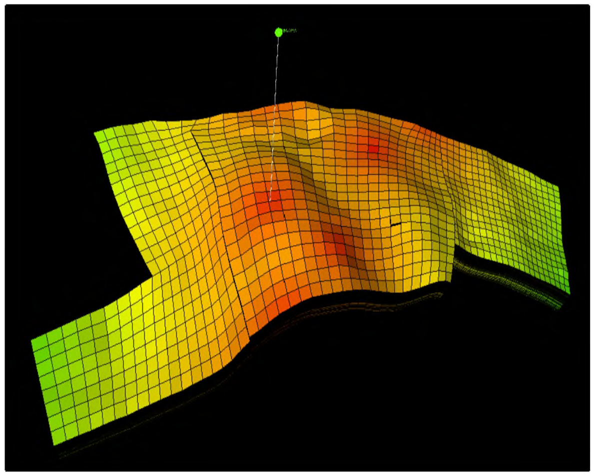

Figure 2.13 Segment Model Showing the Effect of Distance from Well Property.

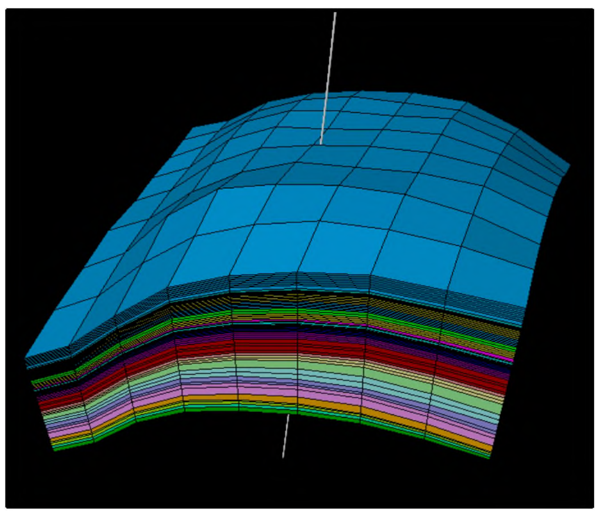

Figure 2.14 The Final Sector Model with Formation Layers.

Table 2.3 The Cell Count of the Models.

| Model | Grid Cells Count |
|---|---|
| *Fine* | 9,600 |
| *Up-scaled* | 4,352 |
| *Refined* | 73,728 |

**2.3.2. Well Data Revision.** The issues with well deviation, perforations, and fracture centralization, which were encountered during the data collection and validation process will be addressed in this section.

The well deviation problem can be solved in two ways, either by importing the deviation survey or by the use of the well path design feature in Petrel, which was the approach used to tackle the issue. By providing the software with depths, azimuth, inclination, and the shape of the directionally drilled well, the software then creates the path in the well passing through the target formations in the model as demonstrated in Figure 2.15.

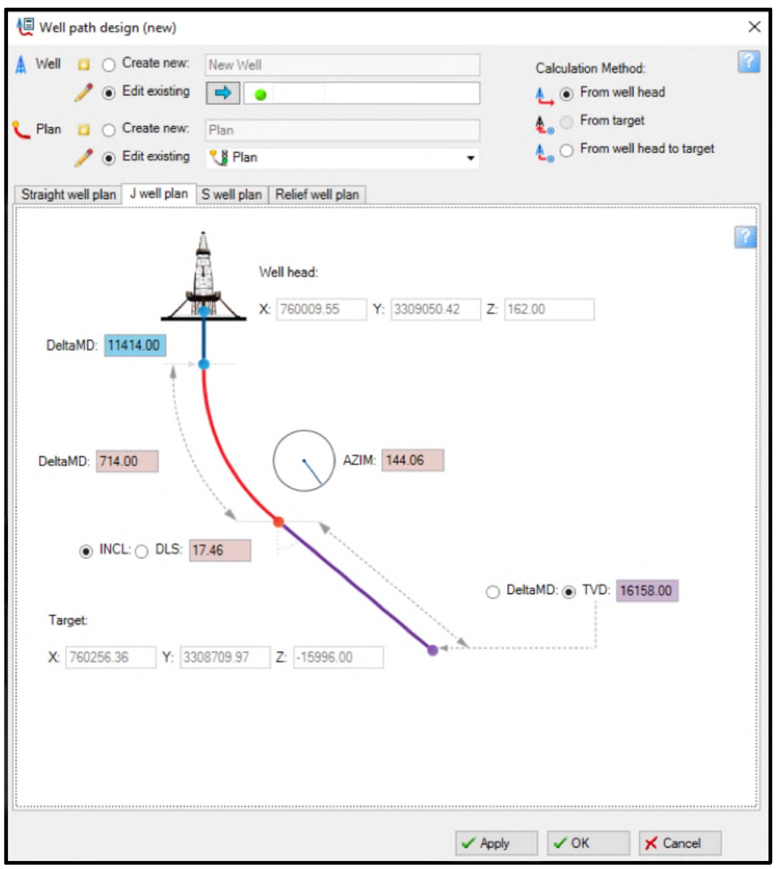


Figure 2.15 Well Path Design Feature used for Well Deviation.

The perforation and fracture interval issues were tackled by simply creating a new well with the revised well perforations from PLT and the fracture interval centralized with respect to it as indicated in Figure 2.16.

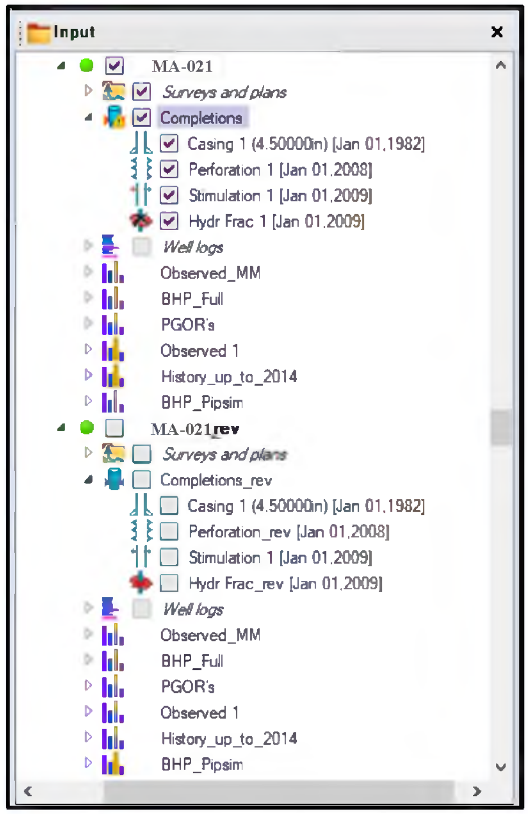


Figure 2.16 New Well with Revised Data.

**2.3.3. Simulation Pre-run.** Before testing the sector model, several parts need to be reviewed in the software to build a simulation case and ensure a smooth simulation run free of errors. The reviewed sections are as follows:

- Fluid model
- Relative permeability curves

- Rock properties
- Development strategy

Many numbers of simulation cases had to be built for the HM process, the created stimulation designs, and the sensitivity analysis. Each case has the matrix and fracture properties, along with sigma which is the controlling factor of the flow between them as illustrated in Figure 2.17.

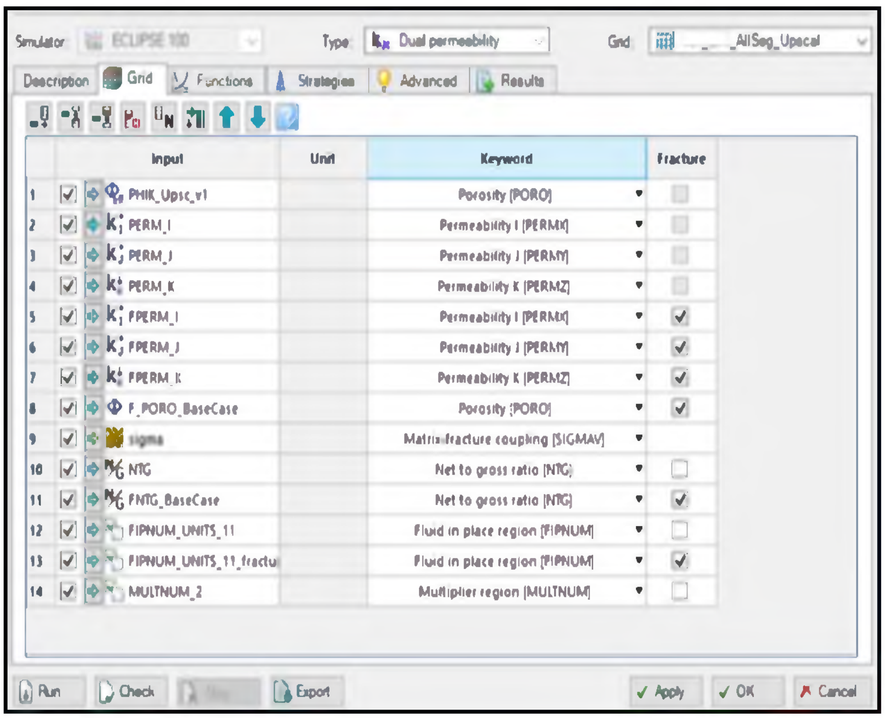


Figure 2.17 An Example of a Simulation Case.

Imbedded into the cases, is the development strategy, where the well conditions are identified and controlled. In addition to that, it contains the well history production data, which have to be matched before moving to the prediction phase as shown in Figure 2.18.

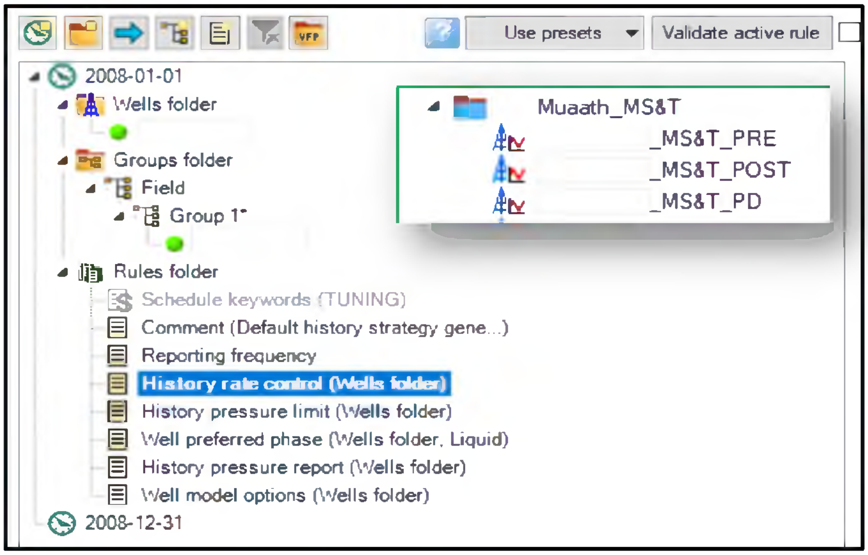


Figure 2.18 An Example of a Development Strategy.

The software introduces two ways to input a stimulation event, one is by simply increasing the KH with a multiplier around the wellbore, and the second is by entering the fracture geometry and conductivity in the well data as indicated in Figure 2.19.

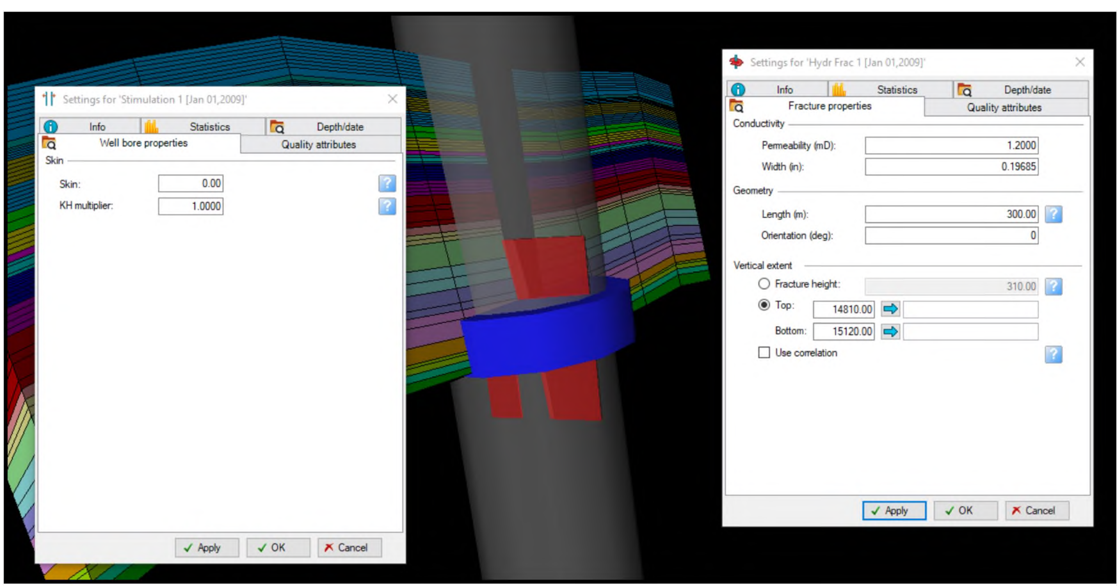


Figure 2.19 Stimulation Events Feature.

**2.3.4. History Matching.** The work done during the HM process was separated into two cases:

- Case_01: history match all the production data (2008 – 20014) to test the model capability of producing the actual production rates during this period as demonstrated in Figure 2.20.
- Case_02: history match the production data (2008 – 2009) to match the production rates prior to the fracture job.

The history production rates and the well-head pressure showed an abnormal trend starting in July 2012. That raised a suspension of unvalidated data that needs to be investigated before running the cases. The reason behind the strange plot was that the team at that time installed a new well-head meter for better reading, but the results were not representing nor acceptable, which forced the team to use back-allocated production data to overcome the issue.

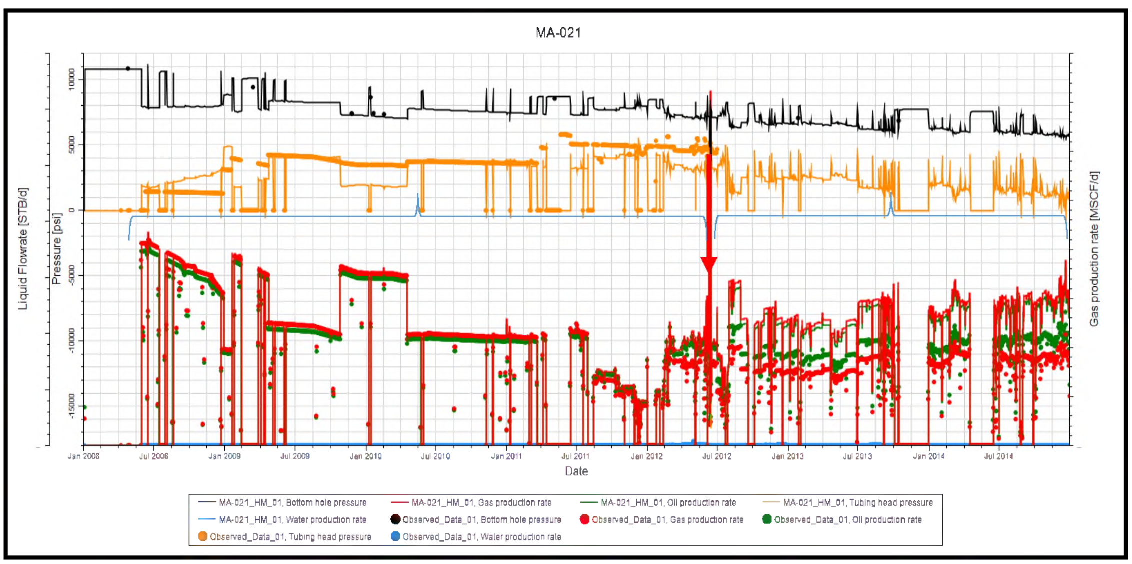


Figure 2.20 Abnormal Trend in Production and Pressure Data in Case_01.

**2.3.5. Production Forecast.** The most interesting part of the study and time-consuming is the prediction. The well performance was set to be predicted for 10 years using the fracture geometry and conductivity taken from the two fracture designs:

- Frac_StimPlan_1D.
- Frac_StimPlan_3D.

**2.3.6. Sensitivity Analysis.** At the beginning of the research, there was no need to perform a sensitivity analysis, but the well performance of the fracture designs shed the light on its importance and valuable contribution in the post-fracture production investigation. Thus, a sensitivity analysis was performed on the well performance for 10 years production period using the following parameters:

- Fracture half-length.
- Fracture height.
- Fracture width.
- Fracture orientation.
- Fracture permeability

# 3. RESULTS

## 3.1. FRACTURE MODELING RESULTS

The following sections cover the results of the fracture modeling part of the study by presenting the outcome from StimPlan.

**3.1.1. Post-Fracture Data Analysis Results.** The results of the study in Table 3.1 are compared with the data analysis results performed by the service company in Table 3.2. The difference in the pressure values goes back to the reason that in our interpretation we used the surface treating pressure instead of the doubted calculated bottom-hole pressure, which was used by the service company.

Table 3.1 Data Analysis Results from StimPlan.

| | | Step Rate Test | | Calibration Test | |
|---|---|---|---|---|---|
| | | *SRT_Decline* | *SRT* | *Calibration_Injection* | *Calibration_Decline* |
| | *Extention Pressure* | | 6319.58 | | |
| | *Extention Rate* | | 9.15 | | |
| | *Closure Pressure (Pc)* | | 3719.42 | | |
| **ISIP Plot** | *ISIP* | 8560.59 | | | 9436.96 |
| **Horner Plot** | *Reservoir Pressure (Pres)* | 2505.64 | | | 2465.25 |
| | *Pumping Time* | 19.3 | | | 18.2 |
| **Square-Root Plot** | *Closure Pressure (Pc)* | 4996.09 | | | 5059.81 |
| | *Closure Time (Tc)* | 1.13 | | | 5 |
| | *Efficiency* | 0.05 | | | 0.19 |
| **G-Function Plot** | *Closure Pressure (Pc)* | 4997.77 | | | 5038.255 |
| | *Closure Time (Tc)* | 1.12 | | | 5.084 |
| | *Efficiency* | 0.051 | | | 0.191 |
| **Barre Plot (G dp/dG)** | *Closure Pressure (Pc)* | 5002.21 | | | 5336.44 |
| | *Closure Time (Tc)* | 1.33 | | | 5.047 |
| | *Efficiency* | 0.059 | | | 0.189 |
| **Type Curve** | *KH* | 310.15 | | | 214.983 |
| | *Permeability (K)* | 3.34 | | | 2.312 |
| | *Reservoir Pressure (Pres)* | 2420.71 | | | 2926.9 |
| **Flow Regimes Plot** | *Reservoir Pressure (Pres)* | 2505.64 | | | 2465.25 |
| | *KH* | 297.75 | | | 105.52 |
| | *Permeability (K)* | 3.2 | | | 1.135 |
| **Friction Plot** | *Closure Pressure (Pc)* | | | 5059.81 | |
| | *Friction Pressure* | | | 3443.3 | |

It was noticed from the values, that the estimation of fracture permeability is around 300,000 mD, which 10 times higher than what StimPlan predicted. That overestimation might give promising production rates that contradict reality, which was witnessed in the post-fracture production test of the well.

Table 3.2 Data Interpretation of the Service Company.

| Step-Rate Test | | | Calibration Test | | |
|---|---|---|---|---|---|
| Bottomhole ISIP | psi | 14,858 | Surface ISIP | psi | 9,321 |
| Estimated Pc. | psi | 14,003 | Bottomhole ISIP | psi | 15,926 |
| Frac. Gradient | psi/ft | 0.93 | ISIP Gradient | psi/ft | 1.06 |
| Estimated K | md | 1.2 | Estimated Pc. | psi | 14,193 |
| Estimated Tf | md-ft/cp | 707 | Frac. Gradient | psi/ft | 0.94 |
| Estimated Pnet | psi | 1,542 | Estimated K | md | 1.09 |
| | | | Estimated Tf | md-ft/cp | 628 |
| | | | Estimated Pres. | psi | 9,595 |
| | | | Estimated Pnet | psi | 1,733 |

Another observation was that our interpreted values from each plot are in line with each other, which raises the credibility of both the model and the results. Although, interpreted data from the Barre plot was not close enough and that is understandable since the plot works better in low permeability formations and high fluid efficiency which is not the case in this study.

**3.1.2. History Matching Results.** In the 1D model, the match was obtained by tuning the leak-off coefficient and stress contrast within the dolomite layers only as shown in Figure 3.1. While in the 3D model, the match was achieved by tuning the parameters in both dolomite and tight carbonate layers as demonstrated in Figure 3.2.

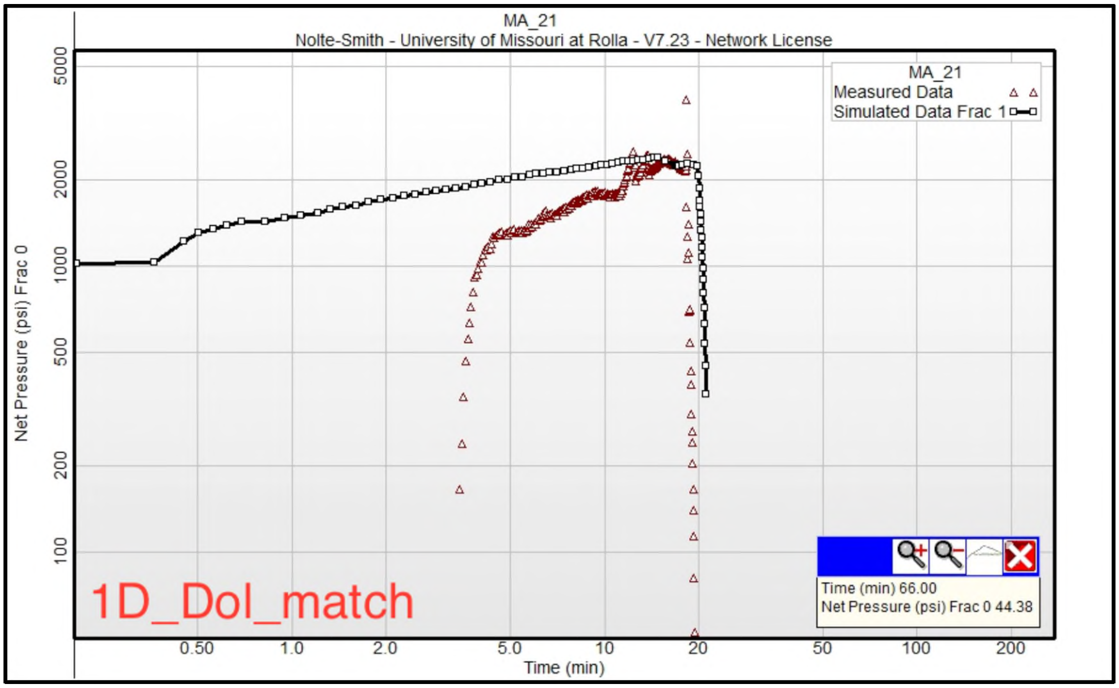


Figure 3.1 Matched Net Pressure Data via 1D Modeling.

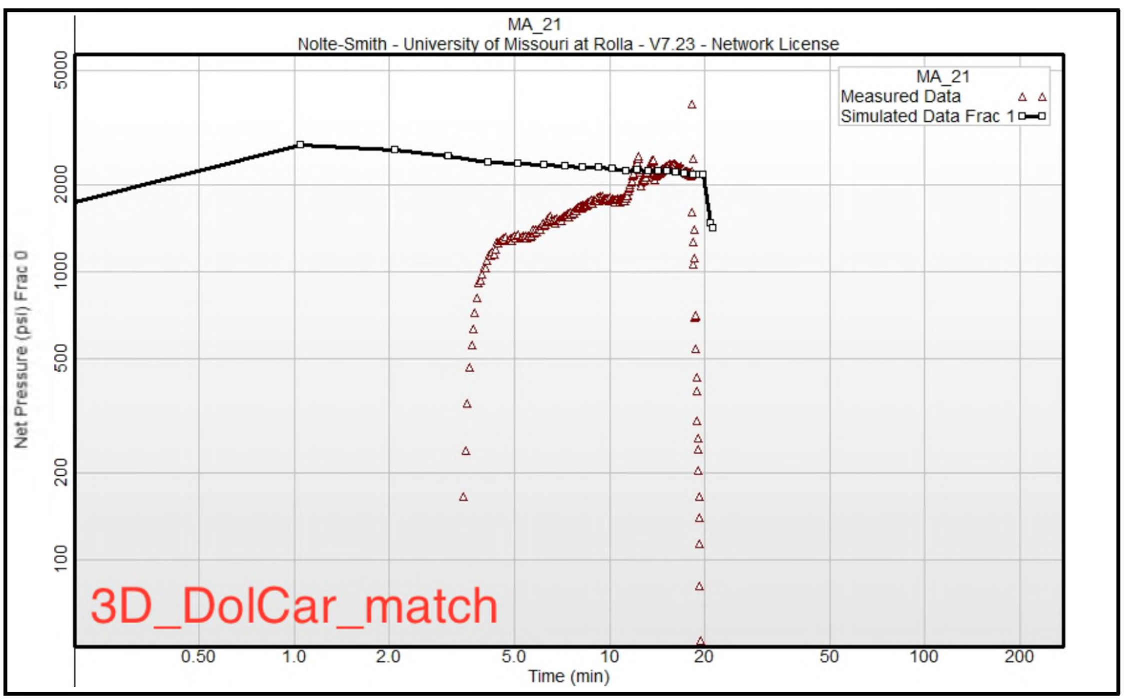


Figure 3.2 Matched Net Pressure Data via 3D Modeling.

**3.1.3. Fracture Designs Results.** Out of all nine fracture designs indicated in Table 3.3, only two were selected to be tested in the reservoir simulation model. That is due to the unfortunate reason of StimPlan not calculating the fracture conductivity in the absence of proppants in the design. Thus, Frac_design_02 results in 1D and 3D models we transferred to the reservoir simulator.

Table 3.3 Summary of Fracture Designs Results.

| Name | Fluid Type | Slurry Volume bbl | Proppant Type | Proppant Conc. ppg | Pump Ratre bbls/min | Fcd | Xf ft | Hf ft | Wf in | Fracture Conductivty md-ft | Fluid Efficiency % | Comments |
|---|---|---|---|---|---|---|---|---|---|---|---|---|
| Frac_design_slb | ClearFRAC_K | 3048 | 20/40 | 0.5 - 1.0 | 20 | 0.25 | 148.8 | 327.4 | 0.29 | 40.9 | 13% | software design \| 1D |
| Frac_design_01 | ClearFRAC_K | 2000 | - | - | 20 | - | 131.2 | 288.6 | 0.27 | - | 14% | no proppant \|1D |
| Frac_design_02 | ClearFRAC_K | 2000 | 20/40 | 1.0 - 4.0 | 30 | 2.02 | 142.4 | 313.3 | 0.31 | 307.7 | 19% | with proppant \| 1D |
| Frac_design_03 | ClearFRAC_K | 1980 | - | - | 30 | - | 142.7 | 314 | 0.9 | - | 19% | no proppant_multi-stages \|1D |
| Frac_design_slb | ClearFRAC_K | 3048 | 20/40 | 0.5 - 1.0 | 20 | 0.14 | 193.1 | 337.9 | 0.25 | 30.2 | 9% | software design \| 3D |
| Frac_design_01 | ClearFRAC_K | 2000 | - | - | 20 | - | 179.3 | 248.7 | 0.24 | - | 9% | no proppant \|3D |
| Frac_design_02 | CleaFRAC_K | 2000 | 20/40 | 3.0 - 10.0 | 30 | 2.07 | 182.5 | 347 | 0.32 | 419.1 | 18% | with proppant \| 3D |
| Frac_design_03 | ClearFRAC_K | 1980 | - | - | 30 | - | 178.7 | 346 | 0.27 | - | 16% | no proppant_multi-stages \|3D |
| Frac_design_04 | ClearFRAC_K+A | 1980 | - | - | 30 | - | 178.2 | 347.9 | 0.27 | - | 16% | acid_no proppant_multi-stages \|3D |

The closer dimensionless fracture conductivity to 2, the more optimum and robust the designs become.

## 3.2. RESERVOIR SIMULATION RESULTS

The following sections cover the results of the reservoir simulation part of the study by presenting the outcome from Petrel and Eclipse.

**3.2.1. History Matching Results.** Two simulation cases went under the HM process. Case_01 showed better HM results after using the new back-allocated production data as illustrated in Figure 3.3, which made it possible to match the abnormal data section.

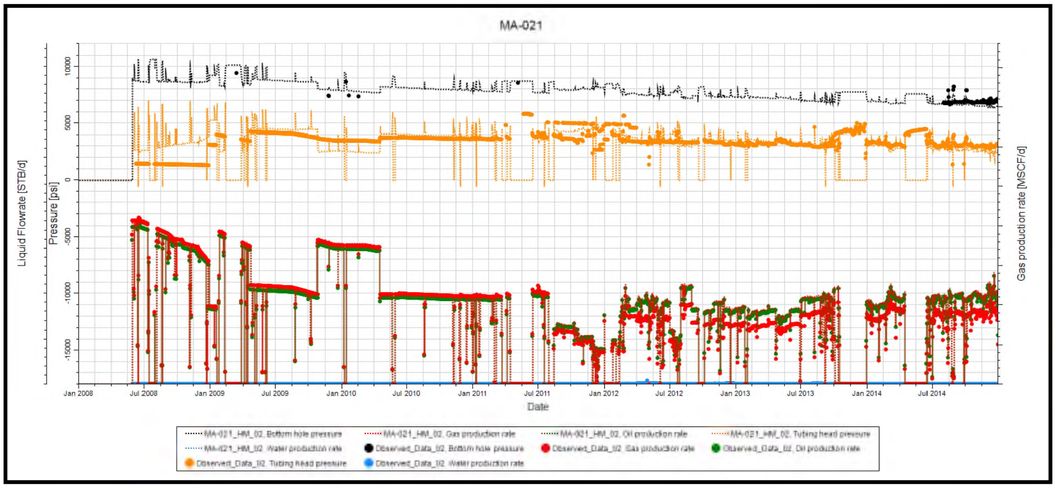


Figure 3.3 History Matched Data of Case_01.

This first match gave the green light to proceed with matching the second case in Figure 3.4, which will be the base case for fracture designs performance predictions.

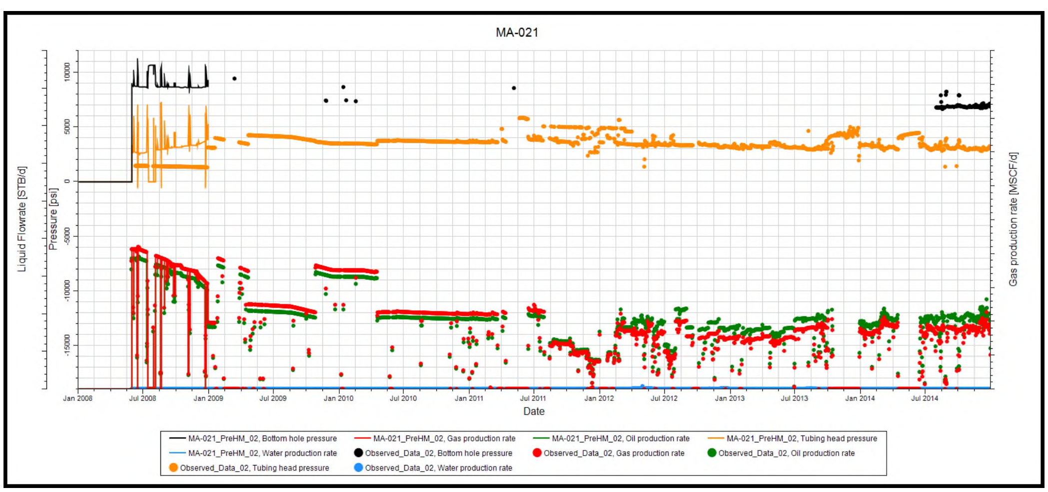


Figure 3.4 History Matched Data of Case_02.

The run of HM in the second case was for 1 year only, which is the period the well was hooked up to the production facility. It is noticeable from the sharp decline in the production data during that period, that the well is depleting quickly and in need for the fracturing job.

**3.2.2. Production Forecast Results.** The prediction results for the two fracture designs were compared with those of the service company. The increase in the cumulative production is barely noticeable from all three designs as demonstrated in Figure 3.5, which is normal due to the long prediction period. But, it also agrees with the fact that the well is not meeting the expected improvement. In addition to that, the close results with the service company design (using a different fracture simulation model and software) give great confidence in our results and the built model.

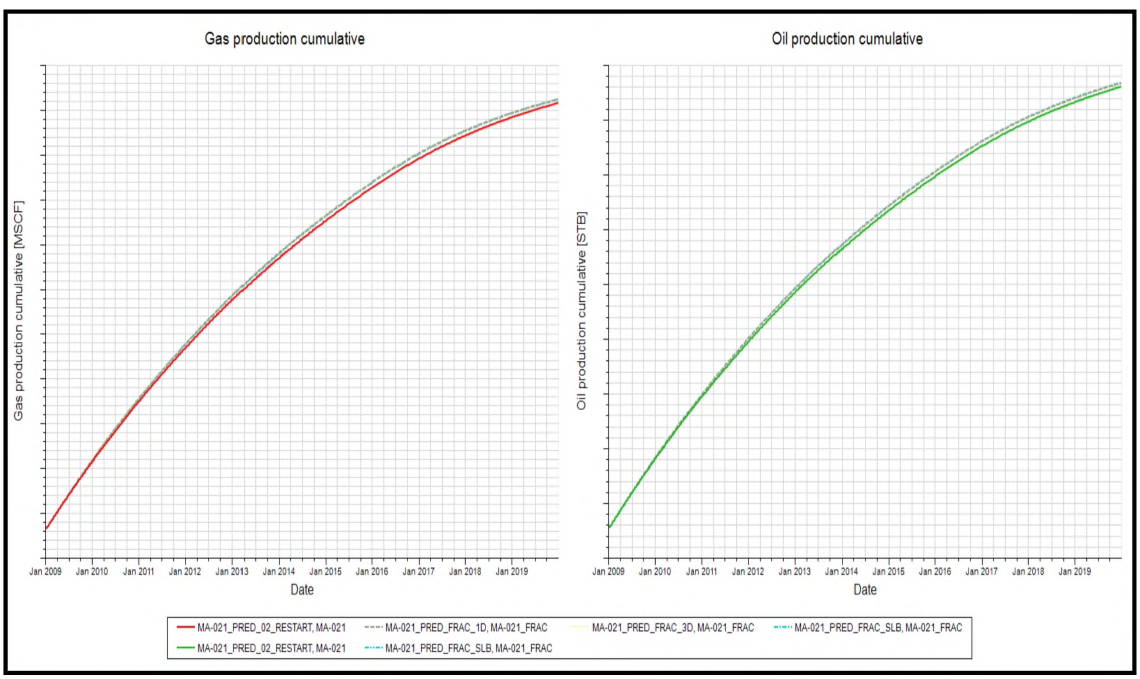


Figure 3.5 Well Performance Comparison of Fracture Designs.

The difference in cumulative production percentage was very close even though the design of the service company gives a 10 times higher value of fracture permeability as shown in Table 3.4, which might be due to the use of acid in their design. That flagged the idea of how big is the impact of each parameter on the results which shed the light on the need for a sensitivity analysis to reveal the magnitude of the impact.

Table 3.4 Parameters and Results of Fracture Designs.

| Frac Design | Kf | Wf | 2 Xf | Orentation | Hf | Gas | Oil |
|---|---|---|---|---|---|---|---|
| | *mD* | *in* | *m* | *deg* | *ft* | *%* | *%* |
| Frac_SLB | 300000 | 0.20 | 91 | 0 | 281 | 0.786% | 0.847% |
| Frac_StimPlan_1D | 29396 | 0.31 | 87 | 0 | 313 | 0.829% | 0.752% |
| Frac_StimPlan_3D | 37400 | 0.32 | 111 | 0 | 347 | 0.830% | 0.753% |

**3.2.3. Sensitivity Analysis Results.** Five parameters with different values were sensitized to examine the effect of each one on the post-production of the well. The results in Table 3.5 show that growing in fracture height will increase the gain in production but to a certain point, where the effect goes in the opposite way. That point could be the point at which the fracture broke through the formation boundaries.

Table 3.5 Sensitivity Analysis Results of Fracture Height.

| Frac Design | Kf | Wf | 2 Xf | Orentation | Hf | Gas | Oil |
|---|---|---|---|---|---|---|---|
| | *mD* | *in* | *m* | *deg* | *ft* | *%* | *%* |
| Frac_25 | 300000 | 0.19685 | 91.44 | 0 | 93 | 0.666% | 0.697% |
| Frac_26 | 300000 | 0.19685 | 91.44 | 0 | 193 | 0.784% | 0.849% |
| Frac_27 | 300000 | 0.19685 | 91.44 | 0 | 293 | 0.754% | 0.848% |
| Frac_28 | 300000 | 0.19685 | 91.44 | 0 | 393 | 0.846% | 0.784% |
| Frac_29 | 300000 | 0.19685 | 91.44 | 0 | 493 | 0.794% | 0.856% |

The impact of increasing the fracture permeability is as expected positive on the cumulative production of the well as illustrated in Table 3.6.

Table 3.6 Sensitivity Analysis Results of Fracture Permeability.

| Frac Design | Kf | Wf | 2 Xf | Orentation | Hf | Gas | Oil |
|---|---|---|---|---|---|---|---|
| | mD | in | m | deg | ft | % | % |
| Frac_20 | 50000 | 0.19685 | 91.44 | 0 | 281 | 0.830% | 0.753% |
| Frac_21 | 100000 | 0.19685 | 91.44 | 0 | 281 | 0.846% | 0.780% |
| Frac_22 | 250000 | 0.19685 | 91.44 | 0 | 281 | 0.785% | 0.848% |
| Frac_23 | 500000 | 0.19685 | 91.44 | 0 | 281 | 0.781% | 0.842% |
| Frac_24 | 750000 | 0.19685 | 91.44 | 0 | 281 | 0.682% | 0.858% |

The percentage of the cumulative production is increasing proportionally with the increase in the fracture width value as demonstrated in Table 3.7.

Table 3.7 Sensitivity Analysis Results of Fracture Width.

| Frac Design | Kf | Wf | 2 Xf | Orentation | Hf | Gas | Oil |
|---|---|---|---|---|---|---|---|
| | mD | in | m | deg | ft | % | % |
| Frac_15 | 300000 | 0.1 | 91.44 | 0 | 281 | 0.785% | 0.848% |
| Frac_16 | 300000 | 0.3 | 91.44 | 0 | 281 | 0.778% | 0.842% |
| Frac_17 | 300000 | 0.5 | 91.44 | 0 | 281 | 0.744% | 0.845% |
| Frac_18 | 300000 | 0.7 | 91.44 | 0 | 281 | 0.628% | 0.846% |
| Frac_19 | 300000 | 1 | 91.44 | 0 | 281 | 0.524% | 0.869% |

The fracture length has a similar positive impact on the performance as shown in Table 3.8. The fracture width, height, length, and permeability, all are taking the same trend in their relation with the gas and oil cumulative production. which is somehow predictable, but what is not expected is how minor is the effect (less than 1%).

Table 3.8 Sensitivity Analysis Results of Fracture Length.

| Frac Design | Kf | Wf | 2 Xf | Orentation | Hf | Gas | Oil |
|---|---|---|---|---|---|---|---|
| | *mD* | *in* | *m* | *deg* | *ft* | *%* | *%* |
| Frac_10 | 300000 | 0.19685 | 50 | 0 | 281 | 0.786% | 0.847% |
| Frac_11 | 300000 | 0.19685 | 150 | 0 | 281 | 0.754% | 0.848% |
| Frac_12 | 300000 | 0.19685 | 300 | 0 | 281 | 0.785% | 0.848% |
| Frac_13 | 300000 | 0.19685 | 500 | 0 | 281 | 0.999% | 0.828% |
| Frac_14 | 300000 | 0.19685 | 1000 | 0 | 281 | 0.768% | 0.669% |

Unlike other parameters, the fracture orientation is not a value that is controlled by increasing and decreasing its value. The angle of orientation is measured with the degree change of the fracture plane, meaning the angle is 0 degree when the plane is perpendicular to the perforations, and 90 degrees when it is parallel to it. The positive and negative values mean that the angle is opening away from the surface when positive and closer to it if negative.

The first observation was the big difference in the impact on the production, which reached up to 3% in the best case where the angle of the fracture plane is at (- 67.5 degrees) as indicated in Table 3.9.

Table 3.9 Sensitivity Analysis Results of Fracture Orientation.

| Frac Design | Kf | Wf | 2 Xf | Orentation | Hf | Gas | Oil |
|---|---|---|---|---|---|---|---|
| | *mD* | *in* | *m* | *deg* | *ft* | *%* | *%* |
| Frac_01 | 300000 | 0.19685 | 91.44 | 45 | 281 | 1.084% | 1.256% |
| Frac_02 | 300000 | 0.19685 | 91.44 | 90 | 281 | 1.016% | 1.287% |
| Frac_03 | 300000 | 0.19685 | 91.44 | -45 | 281 | 2.653% | 2.837% |
| Frac_04 | 300000 | 0.19685 | 91.44 | -90 | 281 | 1.084% | 1.256% |
| Frac_05 | 300000 | 0.19685 | 91.44 | -22.5 | 281 | 0.786% | 0.847% |
| Frac_06 | 300000 | 0.19685 | 91.44 | -67.5 | 281 | 3.041% | 3.305% |
| Frac_07 | 300000 | 0.19685 | 91.44 | -60 | 281 | 2.653% | 2.837% |
| Frac_08 | 300000 | 0.19685 | 91.44 | -70 | 281 | 1.084% | 1.256% |
| Frac_09 | 300000 | 0.19685 | 91.44 | -50 | 281 | 2.653% | 2.837% |

That drastic impact shows the importance of well placing with respect to formation stresses and natural fractures. The right orientation can guide the induced fracture to a better intersection with the formation and the existing natural fractures.

# 4. CONCLUSIONS

The conclusions deduced from the executed work in this study, which aimed to find the reasons behind the underperformance of the well are presented below:

- Investigations showed that human errors in planning and gathering the required data for the stimulation job might lead to poor performance results.
- The geological model in StimPlan showed that the stress contrast between the layers is allowing the induced fracture to propagate vertically, giving more fracture height than the desirable fracture length.
- The sensitivity analysis demonstrated the positive impact of the fracture angle (orientation) on the well long-term performance, by allowing the induced fracture to better intersect with the formation and the existing natural fractures.

# 5. RESEARCH OUTCOME

The advantages of the conducted study and its workflow not only covers the academic area, but also extend to reach the career level in the oil and gas industry. Unfortunately, the acid fracturing design and execution processes are currently handled by service companies, therefore the development teams can benefit from applying the workflow as follows:

- The fracture modeling will give the experience and ability to quality check the fracture modeling simulation (fracture job proposal) provided by the service company.
- Analyzing the fracture job data will provide the capability to quality check the post-fracture analysis reports.
- Cutting the high cost of fracture jobs by handling the design and results analysis.

# 6. FUTURE WORK AND RECOMMENDATIONS

The future work and recommendations are introduced on both academic and career levels:

- Data validation must be carried out before the submission to service companies.
- Geomechanical studies are required to build a representative earth model to give a better understanding and select the optimum well placing for future frac jobs.
- Implementation of a Q/C process on future fracture job proposals and results.
- Tackle the reasons behind the poor well performance discovered in the planning and the operational phases by forming a task force to apply the workflow on all other underperforming wells.
- Pursuing PhD degree:
    - Lab tests on core samples.
    - New fracture modeling accounting for natural fractures effect.
    - Reservoir simulation on multiple wells.

# BIBLIOGRAPHY

Al-Muhailan, M., Juma Shehab, A., Aljarki, J., Sounderrajan, M., Hiray, N., Patil, D., & Desai, A. (2016). First Application of Multistage Completion & Acid Fracturing in Deep Carbonate Reservoirs in Kuwait. Offshore Technology Conference Asia,

Aljawad, M. S., Schwalbert, M. P., Zhu, D., & Hill, A. D. (2018). Guidelines for Optimizing Acid Fracture Design Using an Integrated Acid Fracture and Productivity Model. SPE International Hydraulic Fracturing Technology Conference and Exhibition,

Ben-Naceur, K., & Economides, M. J. (1989). Design and Evaluation of Acid Fracturing Treatments. Low Permeability Reservoirs Symposium,

Delorme, M., Bossie-Codreanu, D., Ben-Gharbia, I., Khebzegga, O., Khebzegga, N., & Ricois, O. M. (2016). Unconventional Production Forecast Needs Integration of Field Hydraulic Stimulation Data Through Fracture Model Calibration and Optimized Numerical Scheme. SPE Argentina Exploration and Production of Unconventional Resources Symposium,

Delorme, M., Oliveira Mota, R., Khvoenkova, N., Fourno, A., & Nœtinger, B. (2014). A methodology to characterize fractured reservoirs constrained by statistical geological analysis and production: a real field case study. *Geological Society, London, Special Publications*, *374*(1), 273-288. https://doi.org/10.1144/sp374.14

Deng, J., Mou, J., Hill, A. D., & Zhu, D. (2011). A New Correlation of Acid Fracture Conductivity Subject to Closure Stress. SPE Hydraulic Fracturing Technology Conference,

Du, S., Yoshida, N., Liang, B., & Chen, J. (2015). Dynamic Modeling of Hydraulic Fractures Using Multisegment Wells. SPE Liquids-Rich Basins Conference - North America,

Jeon, J., Bashir, M. O., Liu, J., & Wu, X. (2016). Fracturing Carbonate Reservoirs: Acidising Fracturing or Fracturing with Proppants? SPE Asia Pacific Hydraulic Fracturing Conference,

Jin, X., Zhang, H., Yin, G., Han, X., & Zhu, D. (2017). Applying the Integrated 3D Acid Fracturing Model Using a New Workflow in a Field Case Study. SPE Symposium: Production Enhancement and Cost Optimisation,

K. Tiwari, B., Al-Sayegh, S., Al-Muraikhi, H., Kumar, P., Cueille, P.-V., & Lislaud, F. (2019). Modelling Hydraulic Fractures in a Full-Field Dynamic Model Using DPDP Simulation Techniques - An Unconventional Approach Applied in a Tight Carbonate Oil Reservoir, Kuwait, Middle-East. SPE Middle East Oil and Gas Show and Conference,

Li, Y., Wei, C., Qin, G., Lu, Y., & Luo, K. (2012). Optimizing Hydraulic Fracturing Design for Shale Gas Production through Numerical Simulations. SPE International Production and Operations Conference & Exhibition,

Lo, K. K., & Dean, R. H. (1989). Modeling of Acid Fracturing. *SPE Production Engineering*, *4*(02), 194-200. https://doi.org/10.2118/17110-pa

McGuire, W. J., & Sikora, V. J. (1960). The Effect of Vertical Fractures on Well Productivity. *Journal of Petroleum Technology*, *12*(10), 72-74. https://doi.org/10.2118/1618-g

Mou, J., Zhu, D., & Hill, A. D. (2010). A New Acid Fracture Conductivity Model Based on the Spatial Distributions of Formation Properties. SPE International Symposium and Exhibition on Formation Damage Control,

Oeth, C. V., Hill, A. D., & Zhu, D. (2013). Acid Fracturing: Fully 3D Simulation and Performance Prediction. SPE Hydraulic Fracturing Technology Conference,

Oeth, C. V., Hill, A. D., Zhu, D., & Sullivan, R. B. (2011). Characterization of Small Scale Heterogeneity to Predict Acid Fracture Performance. SPE Hydraulic Fracturing Technology Conference,

Offenberger, R., Ball, N., Kanneganti, K., & Oussoltsev, D. (2013). Integration of Natural and Hydraulic Fracture Network Modeling with Reservoir Simulation for an Eagle Ford Well. SPE/AAPG/SEG Unconventional Resources Technology Conference,

Ravikumar, A., Marongiu-Porcu, M., & Morales, A. (2015). Optimization of Acid Fracturing with Unified Fracture Design. Abu Dhabi International Petroleum Exhibition and Conference,

Raymond, L. R., & Binder, G. G., Jr. (1967). Productivity of Wells in Vertically Fractured, Damaged Formations. *Journal of Petroleum Technology*, *19*(01), 120-130. https://doi.org/10.2118/1454-pa

Safari, R., Smith, C., & Fragachan, F. (2017). Improved Recovery of Carbonate Reservoir by Optimizing Acidizing Strategy; Coupled Wellbore, Reservoir, and Geomechanical Analysis. Abu Dhabi International Petroleum Exhibition & Conference, Settari, A. (1993). Modeling of Acid-Fracturing Treatments. *SPE Production & Facilities*, *8*(01), 30-38. https://doi.org/10.2118/21870-pa

Sevougian, S. D., Schechter, R. S., & Sepehrnoori, K. (1987). Optimization of Vertical Acid Fractures in Steady-State Flow. SPE International Symposium on Oilfield Chemistry,

Tavassoli, S., Yu, W., Javadpour, F., & Sepehrnoori, K. (2013a). Selection of Candidate Horizontal Wells and Determination of the Optimal Time of Refracturing in Barnett Shale (Johnson County). SPE Unconventional Resources Conference Canada,

Tavassoli, S., Yu, W., Javadpour, F., & Sepehrnoori, K. (2013b). Well Screen and Optimal Time of Refracturing: A Barnett Shale Well. *Journal of Petroleum Engineering*, *2013*, 817293. https://doi.org/10.1155/2013/817293

Terrill, R. M. (1965). Heat transfer in laminar flow between parallel porous plates. *International Journal of Heat and Mass Transfer*, *8*(12), 1491-1497. https://doi.org/https://doi.org/10.1016/0017-9310(65)90034-7

Ugursal, A., Zhu, D., & Hill, A. D. (2019). Development of Acid Fracturing Model for Naturally Fractured Reservoirs. *SPE Production & Operations*, *34*(04), 735-748. https://doi.org/10.2118/189834-pa

Wattenbarger, R. A., El-Banbi, A. H., Villegas, M. E., & Maggard, J. B. (1998). Production Analysis of Linear Flow Into Fractured Tight Gas Wells. SPE Rocky Mountain Regional/Low-Permeability Reservoirs Symposium,

Wennberg, O. P., Rennan, L., & Basquet, R. (2009). Computed tomography scan imaging of natural open fractures in a porous rock; geometry and fluid flow. *Geophysical Prospecting*, *57*(2), 239-249. https://doi.org/https://doi.org/10.1111/j.1365-2478.2009.00784.x

Wu, X., Hill, A. D., Oeth, C., Zhu, D., & Gildin, E. (2013). Integrated 3D Acid Fracturing Model for Carbonate Reservoir Stimulation. OTC Brasil,

# VITA

Muaath Ali Sultan Alansari was born in Kuwait, originally from Failaka Island. He graduated from the University of Missouri-Rolla (UMR) in May 2007, with a bachelor's degree in petroleum engineering. In the same year, he joined Kuwait Oil Company as a petroleum engineer. He worked in data monitoring, production back-allocation, reserves management, well stimulation, reservoir modeling, and simulation. In 2017, he became a senior reservoir engineer in the Jurassic Gas Fields Development Group. In May 2021, he received his master's degree in petroleum engineering from the Missouri University of Science & Technology.